Nanowire Peel-Off for Tandem Solar Cell Applications

Author: Hanna Dickèr

Division of Solid State Physics
Lund University
June 2016

A Master of Science Thesis
Supervisor: Magnus Borgström
Co-Supervisor: Xulu Zeng

LUND
UNIVERSITY

Acknowledgments

My deepest gratitude to my supervisor Professor Magnus Borgstöm for his counsel and encouragement. Thank you for not telling me the answers to every question, as this has stimulated me to find necessary tools for discovering new solutions to problems that seemed impossible. I wish to express my sincere thanks to my co-supervisor Xulu Zeng for his full time guidance in the lab, long discussions about how to proceed when nothing seemed to work and last but not least his patience. I would also like to thank Jovana Colving for the long hours spent with the AFM.

A special thanks to my family which has encouraged me all the way through my studies and always supported my pursuits. I would also like to thank Bob Kaill who supported me in writing and for his belief in me, both outside and in my studies. Finally, my warmest of thanks to John for your love.

Abstract

Nanowires provide interesting features for photovoltaic applications. Materials with desirable band gaps can be combined into heterostructures with very little strain and with a fraction of the material consumption seen in conventional solar devices. Moreover, nanowires show outstanding optical absorption and InP and GaAs nanowire solar cells have been shown to reach efficiencies of 13.8 % [1] and 15.3 % [2].

This project has been done as a step towards building tandem solar cell structures with a top cell consisting of nanowires. A method in which arrays of nanowires with lengths around 2 μm can be peeled off from their native substrate when embedded in a polymer while keeping their array structure and their vertical orientation has been investigated. Moreover, nanowire gold tips were successfully localized using a conductive AFM and imaging of pin-doped InP- nanowires with this method was performed.

Nomenclature

AFM Atomic Force Microscope

ALD Atomic Layer Deposition

BCB Benzocyclobutene

BSE Back Scattered Electrons

cAFM Conducting Atomic Force Microscope

Cu Copper

$\mathbf{E_g}$ Bandgap Energy

FC First Contact ™

GaAs Gallium Arsenide

InP Indium Phosphide

ITO Indium Tin Oxide

LNL Lund Nano Lab

RIE Reactive Ion Etch

Si Silicon

SE Secondary Electrons

SEM Scanning Electron Microscope

Contents

1 Introduction

Nanotechnology has opened up a new path in research in which materials can be designed down to atomic level to obtain desired properties. When the dimensions of an object are extremely small and approach the wavelengths of light or those of electrons, quantisation effects start to emerge and the transport properties are directly influenced by the shape and size of that object. Moreover, as the relative number of atoms existing at the surface compared to in the bulk increases, effects that can otherwise be ignored in a bulk material play an important role in the material properties. For example, does the curvature of a small enough object contribute to a lowered melting temperature. This implies that by engineering materials at the nanoscale, one is able to manipulate material characteristics that would otherwise be a constant property of the bulk material.

The semiconductor industry is moving increasingly towards replacing silicon with materials obtained by combining elements from group III and V in the periodic table, such as GaAs and InP. These III-V materials exhibit higher charge carrier mobilities and thus facilitate high frequency devices [3]. Moreover, they have direct bandgaps giving higher efficiency in photonic devices in contrast to for example silicon which has an indirect bandgap [3, 4]. However, III-V semiconductor materials are rare and expensive and obtaining high quality crystalline thin films is difficult. By replacing thin films with nanowires, where possible, one can save large amounts of such materials.

Nanowires are needle-like structures with diameters between tens and hundreds of nanometers and lengths between a few and some hundreds of micrometers, making them a good approximation of one dimensional structures. Elastic strain relaxation via the surface in epitaxially grown nanowires enables combinations of high quality crystalline materials that would otherwise not be possible due to lattice mismatch. As a consequence, different III-V materials with light absorption in desired wavelength regions are more easily combined. Moreover, less material is required than when growing thin films. This makes nanowires suitable for optoelectronic applications and has opened up the possibility of building highly efficient solar cells. Nanowire arrays with nanowires of 2000 nm length and a diameter of around 200 nm separated by a pitch of 500 nm have shown similar light absorption per area as thin films have shown [1]. Furthermore, nanowires of InP and GaAs have successfully been used to build photovoltaic devices with efficiencies of 13.8 % and 15.3% successively [2, 5]. This has motivated thee Nano-Tandem Research initiative in which the final aim is towards building tandem solar cells in which nanowire solar cells are combined with conventional photovotaic cells for maximized efficiency[6]. To achieve this, one step is to peel off the nanowires from their native substrate for transfer and contact to a planar solar cell.

This project has comprised two separate parts which are presented separately. Firstly, one aim of this project was to develop a method to ensure that peeled off arrays of nanowires keep their array structure and remain vertical. Secondly, electrical measurements on single peeled off nanowires of p-i-n doped InP was done to evaluate the quality of the contacting of the nanowires in a tandem solar cell structure.

2 Background

2.1 Renewable Energy and Solar Power

The effects of fossil fuel emissions are no longer mere speculations, but are effects that can be clearly observed. During the last 40 years the worldwide consumption of resources has extensively depleted Earth's assets and if carbon emission is not reduced we are approaching an ecological footprint of two planet Earths per year [7]. Global energy use is expected to increase quickly within the near future due to growing energy consumption in developing countries. This is partly due to population increase but also a result of the economic and technological development in these regions [8]. If this energy increase can be supplied by renewable sources without increased use of fossil fuels, an otherwise massive increase of carbon dioxide emission can be avoided.

The possible use of solar power is overwhelming when considering that the present annual global energy expenditure is irradiated onto the Earth's surface by the sun during a single hour [9]. While still a very minor producer of energy, the solar energy industry is growing quickly and and while in 2004 it supplied only 0.01% of global energy [10], by the summer of 2015 solar power supplied over 1% [11] which is a hundred fold increase in 11 years. Moreover, after the Paris agreement in 2015 the renewable energy sector is expected and required to grow even faster as the goal for maximum global temperature increase was reduced from 2 °C to 1.5°C [12]. This is indeed a necessity since NASA already reported an average temperature increase of above 1.5°C in Feburary 2016 in comparison to the early industrial age in the late 1800s [13]. It has been predicted that solar power can grow by as much as a factor of 4.9 between 2015 and 2030 if the commitments presented in advance of the Paris Climate Conference are fulfilled [14]. However, a price reduction of solar power is needed to encourage the transition from fossil fuels to renewable energy since solar power is still not cost competitive in most locations around the world [14]. Conventional solar cells today have an efficiency around 20% [10]. Thus competitiveness of solar power is not only limited by the fact that energy can only be harnessed during daylight and needs highly efficient batteries for storage, but also by it's relatively low efficiency and high production costs.

2.2 Photovoltaics

A photovoltaic (PV) cell consists of a pn-junction, very much like a light emitting diode. A junction of positively (p) doped and negatively (n) doped semiconductor material results in a built in potential difference at the joint interface. The region closest to the interface will lose its free charges due to recombination of positive and negative charge carriers and a space charge region, also called a depletion region is created. Incoming photons can excite electrons from the valence band to the conduction band and the charges that are created in the depletion region become separated by the built in electric field and create an open circuit voltage or short circuit current. By introducing an intrinsic region between the p- and n-doped

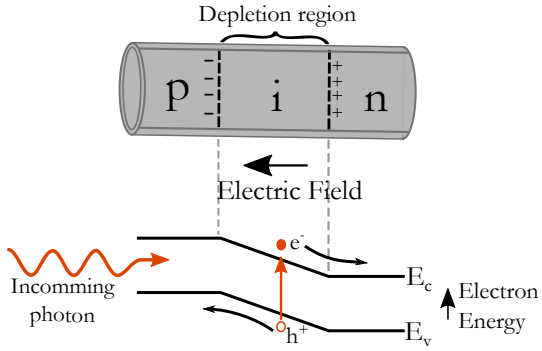

Figure 2.1: Image of the band structure in a p-i-n solar cell device in which an incoming photon with sufficient energy generates a electron-hole pair in the depletion region which creates a current.

segments the area subjected to the built in electric field becomes larger and thus generates more current per device. The working principles for a p-i-n junction is seen in figure 2.1.

A solar cell generates both a voltage and a current as the result of incoming electromagnetic energy. The output voltage is dependent on the built in voltage of the pn-junction which in turn is limited by the semiconductor-material's specific bandgap (E_g) [15]. To obtain a high potential difference one needs to use high bandgap materials. However, only photons with energy $E \geq E_g$ will be absorbed while absorption of photons significantly greater than E_g leads to thermal losses.

The key demands on solar power today are reduced costs, higher reliability and higher efficiency. The most commonly used cells are first generation silicon solar cells [16] requiring 200-500 µm thickness of semiconductor material [17]. Since silicon (Si) is the second most abundant element in the Earth's crust and it is non toxic, the use of silicon itself is not seen as a problem. Industries all over the world have years of experience with Si in fabrication of microelectronics. Silicon however has a indirect bandgap, giving a low absorption coefficient and only makes use of a small range of the solar spectrum.

2.3 New Generation Solar Cells

There is a wide range of possible solutions which could give cheaper and more efficient solar cells. The focus in this thesis is on the building of solar cells which minimize thermal energy loss that occurs as a result of absorption of photons with higher energy than the material bandgap. These cells are one of many in the current development of stacking cells with different bandgaps in order to absorb a wider range of wavelengths, a structure called tandem cells [6, 16, 18]. The theoretical maximum efficiency of a single junction solar cell was calculated by Shockley and Queisser in 1961 to be 33 % [19] while a nanostructured surface can enhance this efficiency to approximately 42 % [20].The tandem structure consists of two or three successive cells and offers a maximum theoretical efficiency of 55.9 % and 63.8 % respectively [18]. The tandem design incorporates a high E_g top cell connected

to a cell with lower E_g via a p^+n^+ tunneling junction. In theory, an infinite number of stacked cells would give the maximum efficiency, but as the number of cells increases the strain between epitaxially grown layers increases, ultimately creating strain damages [15] and therefore tandem solar cells are often limited to two or three successive cells.

III-V semiconductor materials give higher efficiencies in photovoltaic cells due to higher absorption and lower losses as a result of that they commonly have direct bandgaps. Moreover they also provide materials with good lattice match and the bandgap of III-V semiconductors can be tuned by introducing a third element, either from group III or V in the periodic table [15]. This enables a wide range of different bandgap designs and thus favorable characteristics for use in tandem solutions. However, even though less bulk material is required in these cells, the high cost of producing highly crystalline thin films as well as the expensive precursors for materials such as GaAs and InP contribute to a high cost of manufacturing [2]. A nanowire-Based Tandem Solar Cell-project was initiated in 2013 in which one aim is to use arrays of epitaxially grown nanowires to manufacture tandem-structures with high efficiency and decreased material consumption. [6].

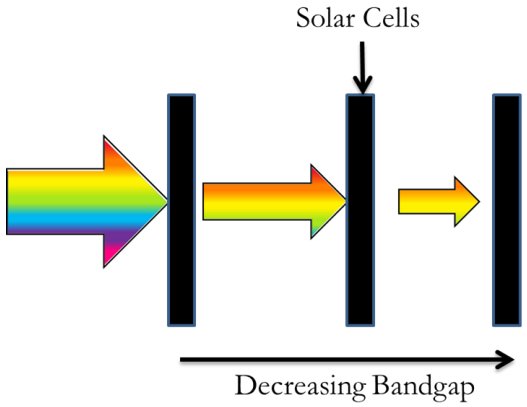

Figure 2.2: Schematic Illustration of the working priciples for a tandem solar cell. Each cell absorbs an individual range of energies form the incoming light, starting with high energy light.

2.4 Nanowires

Nanowires are needle-like structures with aspect ratios that effectively make them one dimensional [21] as they have diameters between a few tens and a few hundred nanometers and lengths between a few and some hundreds of micrometers. An image of such nanowires taken with a Scanning Electron Microcope (SEM) is seen in figure 2.4. This one-dimensionality results in very large surface to volume ratios making them interesting structures for photonic devices.

Nanowires can be made by the "top-down" method in which a bulk material is essentially carved out by lithographic techniques to obtain nanosized structures. However, as the desired dimensions of the nanowires shrink these structures becomes harder to achieve. In contrast, the "bottom-up" approach utilizes epitaxial

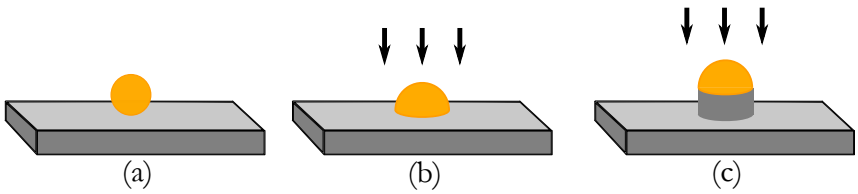

Figure 2.3: Schematic image of the epitaxiall growth of nanowires. (a) Catalyst metal particles are deposited or formed on the substrate. (b) The sample is heated and the seed particle melts. Precursor gasses are introduced. (c) Nucleation occurs at the particle interface and the crystal grows underneath the seed.

growth in which natures way of self assembly of atoms is mimicked to achieve highly crystalline nanowires [22]. Gold particles work as catalytic seed particle for nanowire growth. These seed particles are placed on defined locations on the substrate by using a mask produced by electron beam or nano imprint lithography. Gold is deposited on the substrate which is partially covered by the mask and after the mask is removed by lift off only gold particles remain. By carefully choosing the crystallographic direction of the substrate surface, nanowires can be made to grow vertically underneath the gold particles [4, 21]. Vapor precursors are introduced into the chamber and these diffuse through the catalyst gold particle which is in a liquid state at the pressures and temperatures used and finally a solid, one-dimensional crystal is formed underneath as illustrated in figure 2.3 [22]. As the nanowires are growing it is possible to introduce other gasses to dope the semiconductor or to grow a hetero-structure in which different semiconductor materials are stacked. A SEM image of nanowires grown using this technique is seen in figure 2.4. It is possible to grow nanowires of the expensive III-V semiconductor materials on cheaper substrates such as silicon, increasing the interest of replacing the more expensive thin films of III-V materials with nanowires [1, 2].

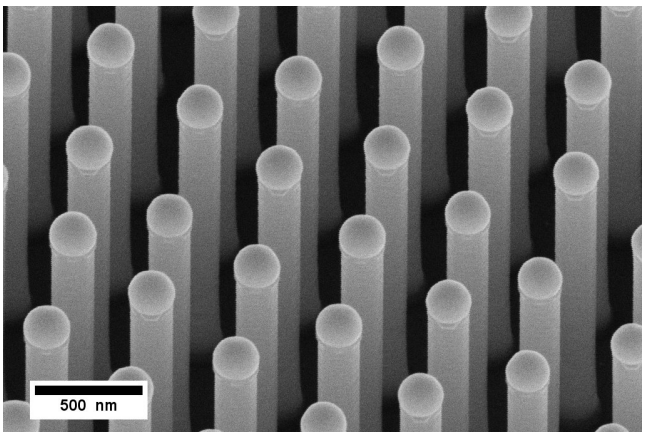

Figure 2.4: SEM image of nanowires of GaInP grown with gold catalyst particles on top of the nanowires. Image courtesy of Xulu Zeng

2.4.1 Nanowire arrays as solar cells

As mentioned above, epitaxially grown nanowires (nanowires) are of interest as one or several of the cells in tandem solar cells. There are several reasons why nanowires are suitable for photonic devices. Elastic Strain relaxation via radial expansion or contraction in nanowire enables combinations of crystalline materials that would otherwise not be possible because of lattice mismatch [23]. As a consequence, materials with absorption of suitable wavelengths are more easily combined. Moreover, it has been shown that nanowire arrays of 2µm long nanowires of InP absorb as much as 94% of the incoming visible light even though only taking up 10% of the volume in the nanowire array [1]. Thus, using nanowires saves large amounts of expensive III-IV semiconductor material in comparison with thin films of the same materials. Furthermore, the nanowires shows good antireflecting properties [4] which are desirable properties for photovoltaic devices [15].

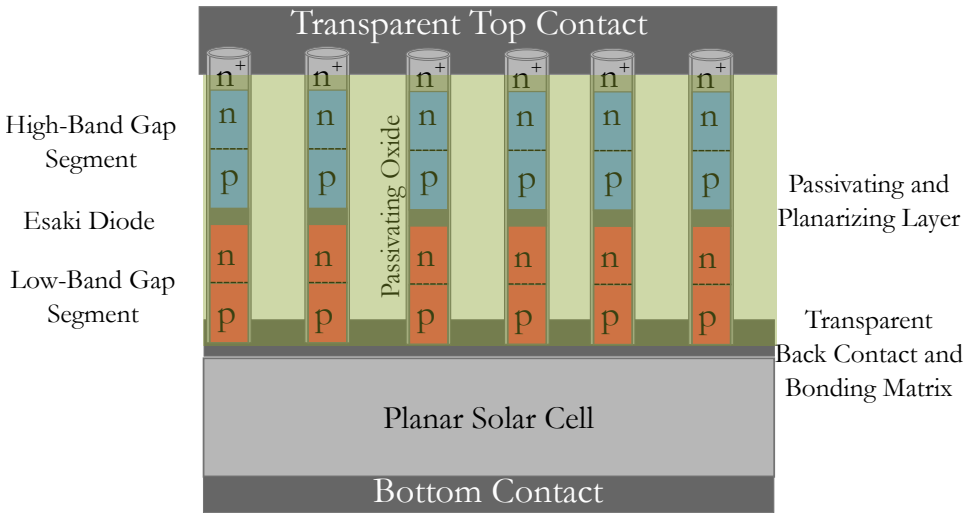

Figure 2.5: Schematic image of the final structure inspired by the structure presented by Borgström in 2014 [24]. Nanowires with a transparent top and back contact are connected to an additional planar solar cell which absorb low energy light.

As mentioned above, nanowires can be grown from a range of III-V materials. Nanowires of InP and GaAs have successfully been used to build photovoltaic devices with efficiencies of 13.8 % and 15.3% successively [2, 5]. These materials do not absorb the low energy light which is absorbed in conventional silicon solar cells but will absorb the high energy light with less thermal losses. The aim is now to connect nanowire solar cells to underlying planar Si- solar cells in order to make tandem cells making use of a wider range of the solar spectrum. An example of such a a design is seen in figure 2.5 in which three layers of solar cells are formed by the heterostructure in the nanowires in combination with the new substrate underneath which works as a solar device as well. The two segments of different bandgaps in the nanowires are separated by a tunneling diode, also called an Esaki diode. An Esaki diode is formed by heavy (degenerate) doping of the p and n-segments that are in contact in sharp transition. The very high doping results in a broken bandgap meaning that the electrons on the n-side is close to aligned with

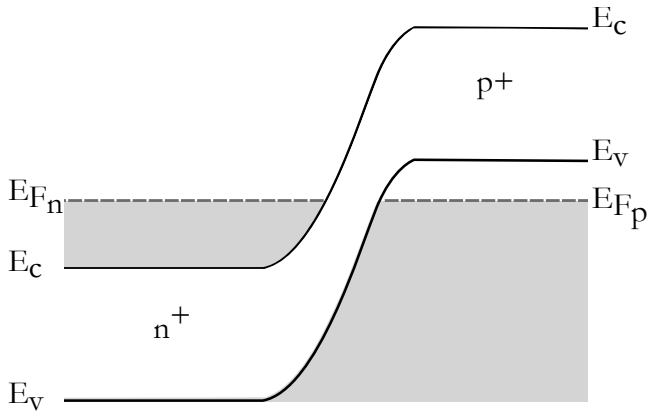

Figure 2.6: Schematic image of an Esaki-diode under zero bias. The Fermi levels are close to aligned which allows for tunneling of charge carriers when the diode is subjected to a bias. The gray area represent energy states occupied by electrons.

the valence band on the p-side and therefore the electrons easily tunnel through the thin depletion region when the diode is subjected to a potential bias, instead of having to overcome the potential barrier between the p- and n-side [25]. An Esaki diode is illustrated in figure 2.6. Research on the incorporation of an Esaki diode into nanowires is conducted at Lund University but will not be explored further in this thesis.

The device seen in figure 2.5 was to be achieved by peeling off of nanowires from their native substrate and transferring them to a new cell. Similar structures in which peeled off nanowires with both top and back contacts have been shown to work well as Light-Emitting Diodes [26].

2.5 Device Fabrication

Prior to this project, nanowires of InP with a length of 2 μm and diameter of 180 nm had been successfully embedded in a polymer film and peeled off from their substrate either using the polymer polydimethylsiloxane (PDMS) or SolOne ™ [1, 27]. These were later replaced by the polymer First Contact ™ (FC) supplied by Photonic Cleaning Industries since neither PDMS nor SolOne ™ could be processed in the clean room due to that processing of these polymers lead to contamination of the tools. FC, which a strip coating otherwise used for cleaning optics and mirrors, has high adhesion to the nanowires and leaves no residues on the surface after peeling. FC contains a solvent component consisting mainly of Acetone and Ethyl Alcohol that evaporates after the solution is deposited. FC Thinner is supplied by Photonic Cleaning Industries as a remover for FC.

Because of the very low viscosity of FC, depositing all of the polymer solution at the same time would give a too thin film with a big area. Therefore a stepwise application is used. First enough solution is dripped to just cover the entire area of the nanowire sample. This is then left to settle for about 15 minutes before a second layer is deposited. FC is typically deposited three times to get a suitable film for peel off which then becomes approximately 2 mm thick. Such thickness was required to enable peel off without cracking the FC film. During previous work

on peel off using FC it had been discovered that when nanowires are grown using a mask of Silicon Nitride (SiN_x) on the substrate the peel off was easier.

The initial process design at the start of this project is seen in figure2.7 and 2.8. Nanowires with a cover of a thin oxide layer wich had been deposited for insulation were embedded in a FC polymer film by dripping a polymer solution which was left to air-dry on the sample. Moderate force was then put on the nanowires from above by manually swiping the polymer-embedded sample using the back of a tweezer. This caused the nanowires to break at the substrate surface. Next, 200-300 nm of polymer was etched away from the bottom side after which 300 nm of metal was deposited on the bottom segments of the nanowires. This contact is here on referred to as back contact. By immersing the bottom segments of the nanowires in metal more support was provided after removal of the polymer and a better electrical contact was intended but has not been measured. The sample was then glued to a silicon wafer using PDMS and the polymer film was removed by immersion in its solvent FC Thinner.

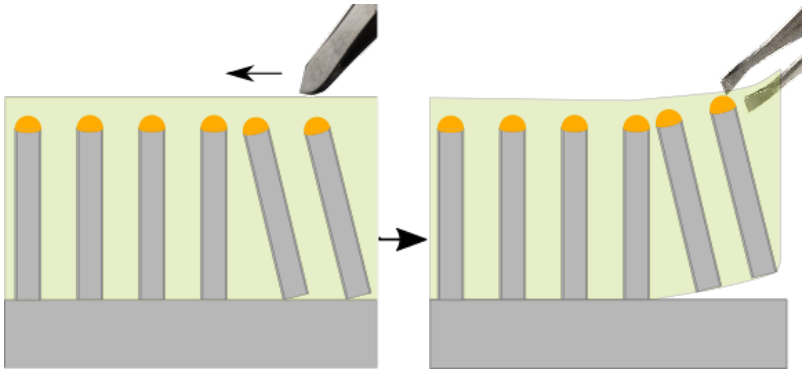

Figure 2.7: Illustration of the process in which nanowires are broken by swiping the back of a tweezer from above by hand, followed by a manual peel off using tweezers.

A planarizing layer was deposited so that a top contact could be applied without short circuiting with the back contact. At the start of the project this was accomplished by depositing a polymer solution onto the peeled off sample by spin coating and etching down to reveal the nanowire tips after dry out. As a final step a transparent contact of indium tin oxide (ITO) film was deposited to obtain an electrical contact to the nanowires which in turn was connected with a gold bonding pad.

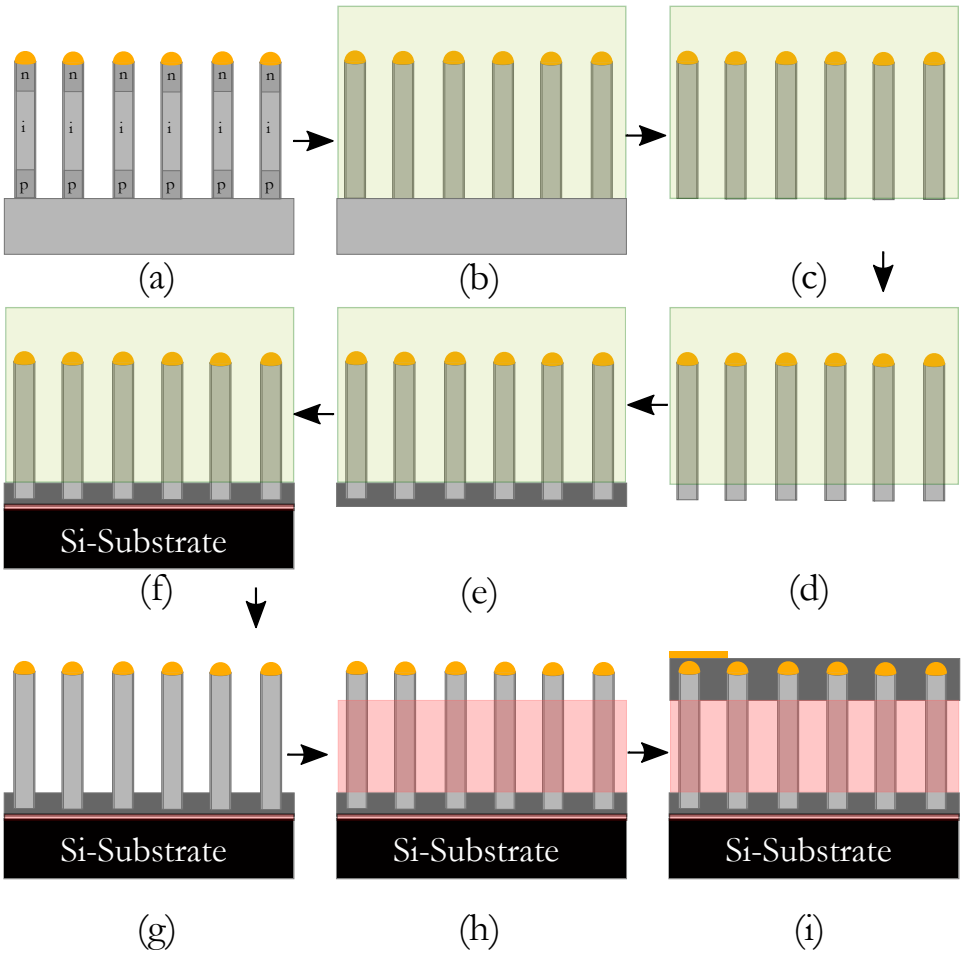

Figure 2.8: Initial process flow at the start of the project. (a) 2µm long nanowires grown with a SiN_x mask covered with a high-k dielectric oxide. (b) Sample immersed in polymer (green). (c) Nanowires were peeled off after the polymer had dried. (d) The polymer film was etched from the back side to reveal approximately 300 nm. (e) Sputtering of metal or ITO contact to the nanowire bases (dark grey). (f) Sample is glued to wafer with PDMS. (g) FC is dissolved in FC-thinner. (h) Application of planar insulating polymer layer (pink). Deposition of ITO (dark grey) and a gold boding pad on top.

2.6 Project Aim

The aim of this project was to examine some of the issues from the previous processing design described above. After dissolving the polymer film in the above design, a large number of the nanowires were tilted or had fallen. The fallen nanowires could indicate a) insufficient support from the metal backing or b) too high force on the nanowires during the rip or c) both. Depositing a thicker layer of metal is a slow and expensive process and the thickness of ITO that can be sputtered in one session in the Lund Nano Lab is limited to 300 nm. Thus, some supportive structure after dissolving the FC was thought desirable. The polymer film that was used for peel off was very thick (1-3 mm) and not feasible to dry etch because the dry etching of such a thick film would take an extremely long time. Due to the poor control during wet etching, a thin supportive film of FC with known thickness could not be left on the sample. Therefore the entire membrane needed to be completely removed before further processing and FC was not suitable as a supportive structure in the final device. Therefore one objective in this project was to create a thin supportive polymer layer that remained after dissolving the FC.

Using tweezers to break the nanowires before peel off by pressing on the nanowires from above was a rather rough method as this was done by hand and the amount of force applied was impossible to control or replicate. An illustrating image is seen in figure 2.7. Furthermore, the tilted nanowires may be a result of a too high lateral shear force on the nanowires during the peel off since the peel off film was stretched greatly during the peeling which sometimes resulted in a permanently elongated and uneven film. At one time previous to this project a supportive mesh had been used but this mesh had been abandoned due to the risk of harming the sample. In the present project a mesh was once more incorporating into the FC-polymer and a second objective of this project was to investigate alternative methods of breaking the nanowires at their base before peel off.

Furthermore the contact between the nanowires and the underlying cell is an important factor when considering how to incorporate nanowires as a cell in a solar device. Therefore a third objective of this project was to evaluate the electrical contact between the nanowires and the back contact by performing probe measurements of single nanowires in a conducting Atomic Force Microscope (cAFM).

3 Nanofabrication

Fabricating structures with nanometer precision sets higher demands on the tools and methods used in comparison to building structures on a macroscopic level. First and foremost, work often has to be carried out in very clean environments, since dust and airborne particles would otherwise contaminate the sample. Moreover, more sophisticated methods of imaging one's sample are needed since high resolutions that cannot be obtained in an optical microscope are required. The following text is an introduction to some of the instruments and methods used in the present project.

3.1 Spin Coating

To obtain thin layers of polymers a method of spin coating can be used. A polymer solution (often referred to as a resist) is dripped onto a sample after which the sample is spun at speeds usually between 1000-5000 rpm. Each polymer solution delivers a different thickness depending on its physical properties such as viscosity and adhesion to the substrate. A spin curve of spin speed against film thickness is a powerful tool when predicting the thickness of a film after spin coating. As seen in figure 3.1 the thickness is material dependent and approaches a constant value at high spin speeds.

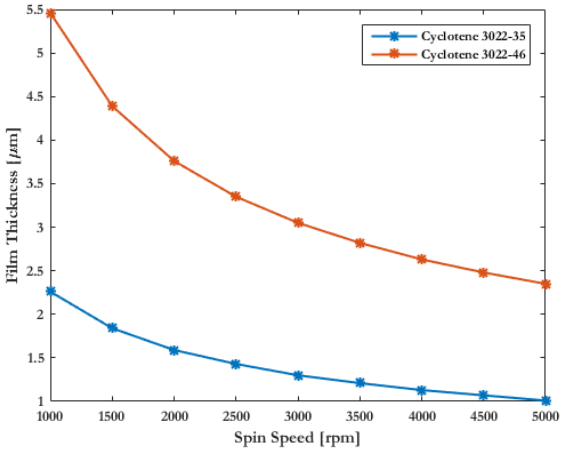

Figure 3.1: Spin Curve for Bisbenzocyclobutene on to a flat substrate

3.2 Atomic Layer Deposition

To achieve thin films with well controlled thickness, Atomic Layer Deposition (ALD) may be used. ALD is achieved by introducing precursor gases one by one into a low pressure sample chamber. The first precursor saturates all available surface sites on the sample after which the first precursor gas is exchanged with the next precursor to allow the two chemicals to react in self terminating reactions. Thus, the film is deposited one monolayer at a time and Ångström thickness accuracy can be achieved [28] . This process is repeated in cycles to obtain a thin film

with a desired thickness. ALD is typically used to deposit very thin films of oxides or metals.

3.3 Sputter deposition

An alternative method of applying films of metal or oxide is to use sputtering. While ALD is a slow process which provides ultrahigh thickness control, sputtering is a faster method with less control of the deposited thickness. Sputtering is a physical vapor deposition method in which sputtering ions (usually Argon ions) are accelerated towards a target in a low pressure chamber. Atoms are ejected from the target as a result of the physical bombardment of the sputtering ions and these atoms travel through the chamber and land on a substrate on which a film grows [29]. In this work, sputtering was used to deposit the back contact of ITO, titanium and gold on the nanowires.

3.4 Reactive Ion Etch

Etching is the term used for removing materials using wet chemistry or a dry method. By using dry techniques one obtains a higher level of control in comparison to chemically dissolving materials through wet etch. In reactive ion etching (RIE) a combination of physical and chemical attack on chemical bonds is utilized. The sample is placed on a large grounded bottom electrode in a parallel plate structure and an RF field is applied to ionize the a gas inside the chamber. The gas is chosen with consideration to the material which is to be etched. Charged ions bombard the sample due to the low pressure (<500 mTorr) and the large grounded electrode [29]. As a result, the sample is physically sputtered by ions at the same time as it is under chemical attack from the gaseous radicals [30]. The etching is anisotropic, meaning that there is a strong tendency of removing material in one specific direction, in this case the vertical. However, the amount of anisotropy depends on the settings used in the RIE. The etch rate is determined by the chemical composition of the gases and the etched material as well as by the sample size, gas flow, pressure and power.

3.5 Scanning Electron Microscopy

SEM is a commonly used microscope used to study features in the nanometer and micrometer range. Instead of an optical beam the SEM utilizes an electron beam which is scanned over the surface to obtain an image.

The minimum feature that can be resolved in a microscope is proportional to the wavelength of the probing beam as given by the Rayleigh criterion [31]. Similar as with light, which can be described as either photon particles or electromagnetic waves, electrons can be described as both particles and waves. The wavelength of visible light is between 400-700 nm while the wavelength of electrons in a SEM accelerated by 10 kV is approximately $\lambda \approx 10$pm [31] giving the electron microscope a significantly higher resolution. The beam is focused into a very small area

of approximately 10 nm which contributes to the high resolution since the signal originates from a well-defined location.

When the electron beam hits the surface there are several resulting signals that can be processed by a detector. Some electrons are scattered back without any loss of kinetic energy, a process named elastic scattering. These electrons are called back scattered electrons (BSE). Simultaneously, some beam electrons may give away energy to the sample through inelastic scattering, giving rise to various signals. One such signal is secondary electrons (SE) which originate from loosely bound electrons in the outer atomic shells in the specimen. This process also leads to X-ray emission that can be useful for spectroscopic analysis.

BSE originate from a large interaction volume inside the sample and the probability of elastic scattering increases monotonously with atomic weight and decreases with beam energy. Thus, an image giving chemical contrast is supplied by this signal. The SE signal on the other hand is emitted from a confined volume very close to the surface since SE are limited by their low kinetic energy below 50 eV [32]. The probability of emission of SE is determined by the depth into the sample, z, and the mean free path of electrons, λ [32]:

$$p \propto e^{\frac{-z}{\lambda}} \tag{1}$$

Since the mean free path of electrons is in the Ångström range, the surface signal is very strong and the SE are very useful when imaging a surface. The imaging of the sample is dependent on transport of electrons which are easily scattered by gases. Thus, vacuum is required to obtain an image. Moreover, the SEM is more suitable for imaging conducting samples since an isolator is unable to transport away electrons and thus isolators quickly get a charged surface which is hard to image. In this project, a Hitachi SU8010 and a LEO 1560 are used to image secondary electrons.

3.6 Atomic Force Microscope

An Atomic Force Microscope is an imaging microscope in which a very sharp tip is scanned across a surface and topological changes are detected by deflection of a laser beam from the back of the probe to reconstruct an image. An AFM works either in contact, tapping or in non-contact mode with the sample. In tapping mode the tip oscillates above the sample and when in close proximity to the sample the frequency of oscillation of the tip changes due to van der Waals interactions. In non contact mode the feedback system monitors the probe height to keep it at a constant distance from the sample surface. In this case the deflection of the probe due to van der Waals forces is read and the height is monitored accordingly. In contact mode the probe touches the sample and a feedback loop is used to keep a constant deflection of the cantilever and thus a constant force between the probe and the sample. All of these three methods result in a topological image of the sample. The best resolution is obtained in contact mode [33] since the feedback control is very sensitive, allowing for resolutions down to 0.1 nm [33]. However, this mode is problematic for two reasons. Firstly, it is the slowest mode and secondly the probe easily crashes into the sample if there are steep changes in topology.

The AFM requires very little surface preparation, gives high resolution and is a rather easy tool to use. However, to obtain high resolution images the quality of the probe is crucial and the scanning is slow. The kind of tip and cantilever used is determined by the scanning mode and the type of sample imaged. Piezoelectric materials are used to accurately control the position of the sample beneath the probe but since the probe needs to be changed manually between modes an exact location on the sample cannot be stored in between scans with different modes.

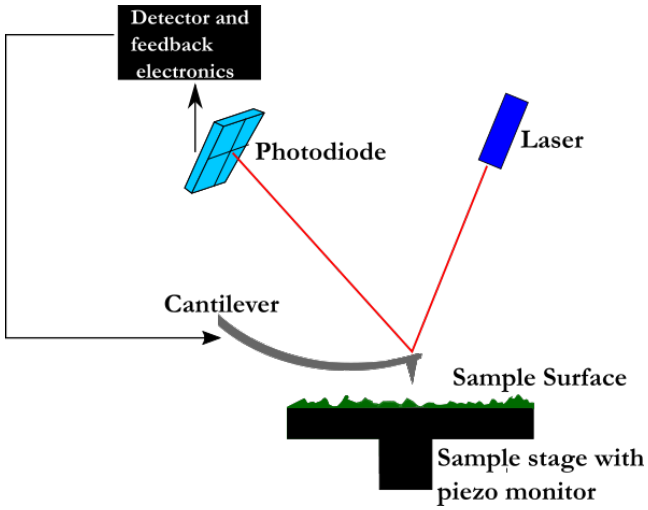

Figure 3.2: Schematic image of the working principle of an AFM. A very sharp tip is raster scanned across the sample. The interactions between the tip at the end of the cantilever and the sample surface is read by the change in position of the laser beam on the photo diode.

If using a conductive probe and electrically connecting the sample to the sample stage one can preform conductive AFM (cAFM). In this mode a voltage is set between the probe and the sample stage and a resulting current is measured which

allows for current mapping of the sample. Moreover one may chose a point on the sample and ramp the voltage between the probe and the samples, obtaining a current against voltage plot at that location. This allows for comparison of the diode characteristics of individual nanowires. In this project, peeled off nanowires were imaged in a cAFM. Similar work as been done by other groups to characterize the electrical properties of nanowires [34, 35] but had not been conducted on the nanowires of interest in this project before.

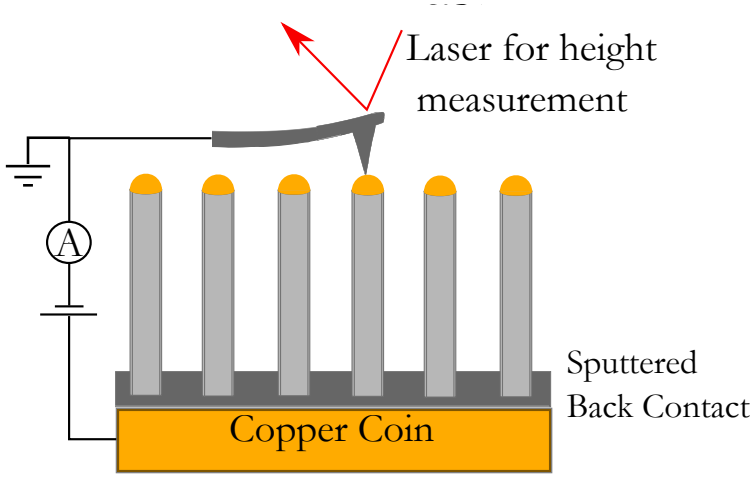

Figure 3.3: Setup used for imaging nanowires in cAFM. A voltage is set between the back contact and the gold tips via the cAFM-tip which is set to contact mode. A current is measured to obtain IV characteristics.

4 Nanowire Peel-Off Development

Due to the nature of this project the method, results and discussion for each step in the experiments will be presented chronologically since the choice of methods have been a consequence of the results obtained from previous work. To ensure that all nanowires are standing straight after peel off this project aimed at developing a design that includes the transfer of nanowires with a supporting polymer film. This supportive film was not to be etched away completely as was FC. Moreover, this film was to be deposited before peel off in contrast to the initial design in which a planarizing layer was spun on the sample after FC had been removed. The nanowire samples used in the following procedure are approximately 2 μm long InP nanowires with a diameter of 180-200 nm and with a 500 nm pitch. The nanowire samples are typically 9x11 mm big. InP nanowires are used due to the ability of growing and doping InP nanowire at Lund Nano Lab. However, due to a limited number of samples, some samples with an uneven distribution of wires with varying diameters had to be used.

To achieve a working solar cell, the gold particle needs to be etched away since it otherwise increases the reflectance of the nanowires. However, the samples worked on in this project were never used for photovoltaic measurements. For the sake of the development of the process design, the etching of gold was not done since the gold particle itself does not affect the other processing steps.

4.1 Deposition of a Supportive Polymer Layer

In order to create a supportive polymer film for the nanowires, the nature of the polymer solutions that were to be spun onto the substrates with nanowires were investigated. The aim was to apply a supportive layer in such a way that the nanowires remained vertical while the film thickness could be well controlled. Three possible ways to deposit a thin polymer layer using spin coating were considered and are illustrated in figure 4.1. a) A polymer solution can be spun to such a thickness that it covers the nanowires completely and then be etched back using RIE to obtain the desired thickness. b) The solution can be spun to a desired thickness directly if it has a suitable viscosity and adhesion to the sample. c) A third scenario is that a desired thickness is achieved by spinning while the polymer builds up and covers the walls of the nanowires. If the polymer solution has low viscosity but high adhesion to the wires, the third alternative was expected as a result of capillary effects. If that is the case, RIE may be used after the spinning to eliminate this buildup. It was quickly discovered that the first and third alternatives were achievable but that none of the polymers used in this work could be spun directly to a perfectly flat layer that covered a partial length of the nanowires. The scenario illustrated in figure 4.1 c. was only seen when depositing Poly(methyl methacrylate) (PMMA) which is explored further in section 4.3.2.

There were several demands set on the supportive layer that had to be met by the chosen polymer. First, the polymer solutions needed to have low enough viscosity and an adequate spin curve to penetrate between the nanowires and give a suitable thickness. Moreover, it needed to be flexible and slightly elastic, in order

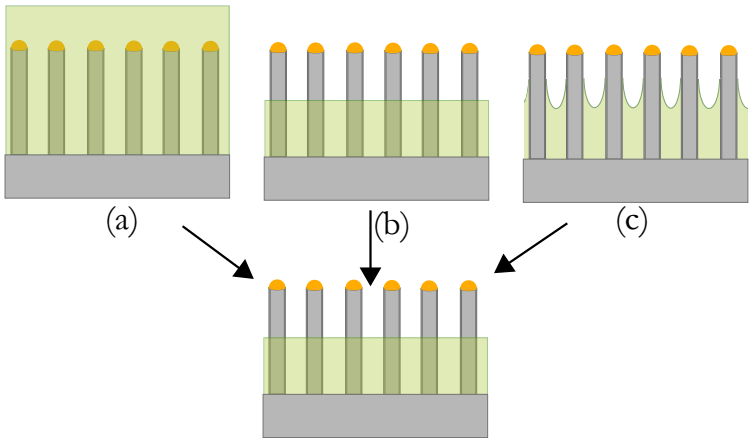

Figure 4.1: Illustration of the deposition of a thin layer of a polymer. (a) A thick, flat initial layer is etched down to the desired thickness. (b) The desired thickness is obtained directly. (c) A layer close to the desired thickness is obtained but with some polymer climbing on the walls of the nanowires.

not to crack during peel off. Finally, optical transparency is required for solar cell applications as well as chemical resistance to the FC Thinner so that FC Thinner can be used to remove FC without dissolving the supportive layer. Three polymers where initially considered as supportive middle layers.; Benzocyclobutene (BCB) and the photoresists S1813 and Tu7. In the following text the choice of supportive polymer solution is motivated and the procedure used to obtain adequate films is explained.

4.1.1 Spin coating onto nanowire samples

Since the samples onto which polymer solutions were spun, consisted of vertical nanowires the thickness of the solutions correlated poorly with the spin curves and higher speeds were required to obtain the desired thickness of the polymer films. It was quickly discovered that there was a variation in thickness of the polymer film across the nanowire sample. At the center of a sample this variation was within $\pm$ 100 nm. However, due to edge effects during spinning the thickness was much higher at the edges and could be several hundred nanometers thicker than in the center. Thus, better results were obtained on larger samples and the following results are from the center of such samples.The final settings are later summarized in table 1.

Tu7 is a photoresist, meaning that the physical properties of the polymer are changes after exposure to ultraviolet (UV) light. Tu7 becomes chemically stable after treatment of Ultra Violet (UV) light and is therefore called a negative photoresist. Moreover, it has an optical absorption below 0.1 % at wavelengths above 350 nm. The polymer solution is supplied by Obducat who do not disclose the chemistry of their product. However, Tu7 consists of a mixture of an epoxy and a salt, dissolved in a Phenyl Methyl Ether. It is recommended by other users at Lund Nano Lab as a possible material to incorporate in a solar cell structure and as a supportive layer for the nanowires due to its flexibility and chemical stability.

No official document giving the spin curves for Tu7 is available. Instead, the parameters were suggested by other users of LNL. Thus, Tu7 was spun on as grown nanowires at 3000 rpm for 60s after which the sample was soft baked. This was followed by UV curing using soft UV and a post bake. From inspection in the SEM it was confirmed that the polymer film was approximately 2 μm and just covered the nanowires.

Micoposit ® S1813 is a positive photoresist supplied by Shipley Company that becomes soluble in it's developer (Micoposit ®. MF-319®) after exposure to UV light. It is a propylene glycol monomethyl ether acetate and it is promoted as having excellent adhesion and coating uniformity [36]. Moreover, it is transparent to wavelengths longer than 450 nm [37] and is regularly used in the clean room. According to the spin curve for S1813, a spin at 2000 rpm for 60s gives a thickness of approximately 2 μm [36]. However, as mentioned previously higher speeds were needed for spinning on nanowire samples. Moreover, a more uniform film was achieved at higher spin speeds [36]. Thus, 3000 rpm was tested and judged as an adequate speed after which the polymer was soft and hard baked. This gave a coating that was was almost completely flat over the entire sample except at the outermost corners where some solution built up during spinning. The film was approximately 2 μm.

Benzocyclobutene (BCB) has previously been used for similar applications as a planarizing layer between a top and back contact in a nanowire solar cell device[2]. Moreover, BCB is 99% optically transparent [38] and is often used as a dielectric in microelectronics. Cyclotene ™ is the trade name of the BCB supplied by Dow Chemical Company Limited. Spinning Cyclotene ™ 3022-35 at 5000 rpm for 60s is a general procedure in LNL to obtain a flat polymer layer that just covers the nanowires. Thus, these settings were used to cover samples of as grown nanowires after which it was soft baked followed by a hard bake using rapid thermal annealing. From inspection in the SEM it was confirmed that the polymer film was approximately 2 μm and just covered the nanowires.

Table 1: Settings used during spin coating of polymers for the supportive layer. The procedure can be followed through the settings that are presented in the chronological order from left to right. T is temperature.

Polymer solution	Spincoat: Speed (rpm)/ Time(s)	Soft Bake: T(°C)/ Time(s)	Hard Bake: T(°C)/ Time(s)	UV-treatment: Wavelength (nm)/Time(s)	Postbake: T(°C)/ Time(s)
Tu7	3000/60	95/60	-	365/25	95/120
S1813	3000/60	90/60	200/1200	-	-
BCB	5000/60	120/ 60	250/900	-	-

4.1.2 Etching the polymer films

When a uniformly thick polymer layer could be deposited through spin coating onto the nanowires this film was to be etched down by using RIE to make the supportive polymer film approximately 1 μm hick. The rate of etching in RIE is determined by numerous parameters. Pressure, gas flow and power can be tuned to achieve a change in rate. However, the size and shape of the sample also play important roles since edge effects may be strong [39]. The RIE in LNL is supplied with a thickness monitor. A laser beam is shone onto the sample and the reflected signal is either amplified or reduced due to interference between the beam reflected on the bottom interface between the film and its substrate and the one reflected on the top of the film. By calculations one can estimate the etched thickness from the changes in the amplitude of the reflected signal. However, the thickness monitor gave no conclusive signal when used on samples with nanowires.

Since no in-situ measurements of the film thickness during RIE were possible, the etching rates used to determine the time needed for etching down the intended thickness where obtained from other users of Lund Nano Lab and published work [40]. Thin amounts were etched at a time and the samples were inspected with the SEM in between etching sessions. The approximate etching rates for several polymer films on various samples are summarized in table 2 which demonstrates the large variations in etching times for each polymer. Due to the unpredictability of the time needed for etching only small amounts could be etched at a time and generally several sessions of etching were needed. S1813 resulted in a polymer film that could be etched with the highest degree of control.

Table 2: Settings used and resulting etching rates of polymer films in RIE.

Polymer solution	O_2-flow (sccm)	CF_4-flow (sccm)	Power (W)	Pressure (mTorr)	Rate (nm/s)	Std. dev.
Tu7	40	-	40	150	0.5	0.3
S1813	15	-	75	300	1.5	0.3
BCB	70	10	150	250	34.0	12.9
FC	15	-	50	300	1.37	0.9

4.1.3 Resulting Supportive Layers

Thin supportive layers of Tu7, S1813 and BCB were obtained by spinning with the settings presented in 4.1.1 and etching down the film according to table 2 thin polymer films of around 1 μ thickness which immersed the nanowires were obtained.

Tu7

The SEM images showed that a uniform film of Tu7 could be created. However, a large amount of Tu7 residues remained on samples that were etched in RIE after UV-treatment. Still, Tu7 was judged as an adequate polymer to use as a supportive film for the nanowires.

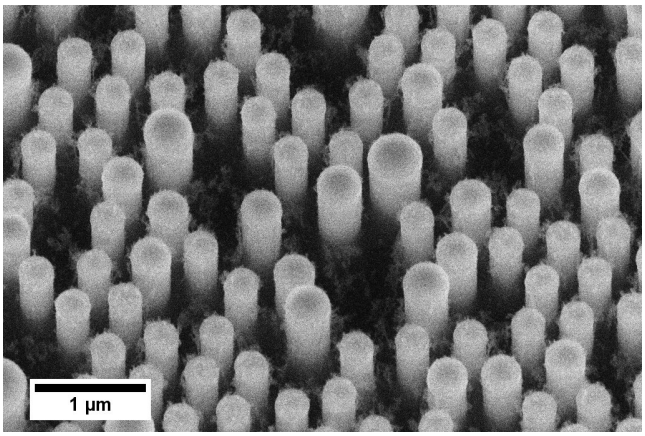

Figure 4.2: SEM image of nanowires in a Tu7 film after RIE etching to reveal the nanowire tips.

S1813

The results showed that S1813 may be adequate as supportive polymer. It could be concluded that S1813 could be etched with rather accurate predictions of removed thickness. The film was uniform after etching, as long as no nanowires where missing from the array. At locations where nanowires were missing due to the uneven array the film was approximately 100-200 nm thinner.

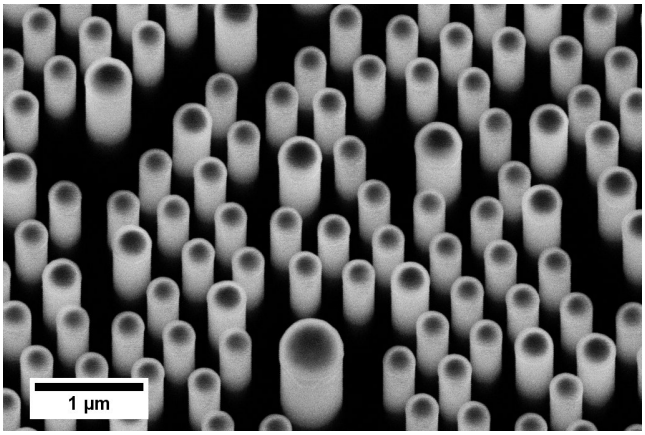

Figure 4.3: SEM image of nanowires with an oxide coating in a S1813 film after RIE etching to reveal the nanowire tips.

BCB

After etching down BCB with the settings according to table 2 a uniform layer of BCB was formed, but as can be seen in figure 4.4a there is a ring formation seen around the nanowires. It was suggested that these rings were resulting from poor adhesion of BCB to the nanowires giving rings already during the spinning of the polymer. This would lead to an increased etching rate at the surface of the

nanowires as the plasma penetrated between the nanowires and the film. Such rings around the nanowire have been observed by other groups in Lund Nano Lab as well as by external researchers [41].

To increase the adhesion of BCB to the nanowires, as grown nanowires were covered in oxide using ALD. Nanowires where covered with 300/50 Å of SiO_2/AlO. Nanowires with this coating will be referred to as oxide coated nanowires in the rest of this paper. Since oxide coating of the nanowires was to be used in the final structure as a dielectric layer, this step had to be implemented in the final processing method in any case. The AP3000 adhesion promoter supplied by Dow Chemical Company Limited is specifically designed to enhance the adhesion of BCB to various surfaces. Thus, using the same settings as above, BCB was spun and post-treated onto a nanowires sample with oxide coating and onto a nanowire sample with both an oxide coating and with AP3000 that had been spun on prior to BCB.

The resulting polymer films after RIE are seen in figures 4.4b and 4.4c. On all samples with BCB, ring formation due to poor adhesion and uneven etching was observed. This ring formation greatly limits the predictability of the film quality obtained after coating and etching since it cannot be controlled. If BCB is to be used in combination with other polymer films or if metal is to be sputtered on top of the samples it will probably not be possible to perfectly describe the final structure.

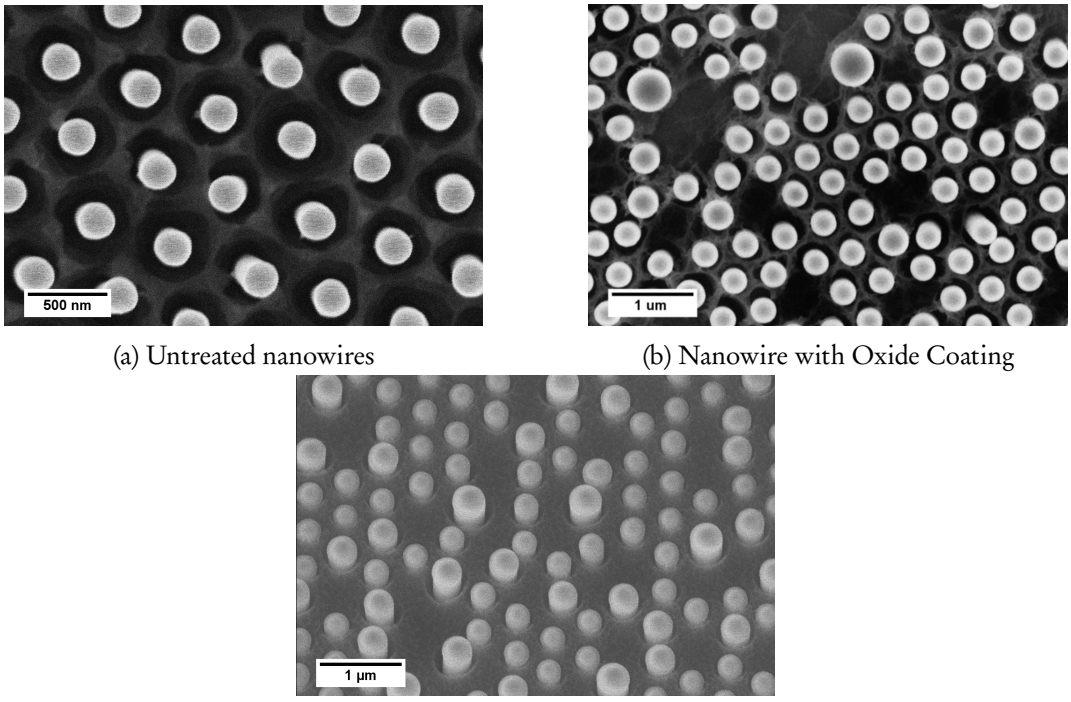

(a) Untreated nanowires

(b) Nanowire with Oxide Coating

(c) Nanowires with oxide coating and adhesion promoter

Figure 4.4: SEM images of samples with nanowires of different surface treatments prior to deposition and RIE of BCB.

4.2 Two Layer Design

We investigated the possibilities of producing a design with two layers of polymers to create a final structure with a supportive polymer film around the nanowires. The aim was to use a first layer which adheres well to the FC covering approximately 1µm of the nanowires for support. After peel off, this supportive layer was to be etched back around 300 nm to reveal the backside of the nanowires, but the remaining film would remain in the final structure as support after FC was dissolved. The intended process flow can be seen in figure 4.5. The polymer films obtained above motivated the use of either Tu7 and S1813 as the bottom supportive layers and FC as the top layer.

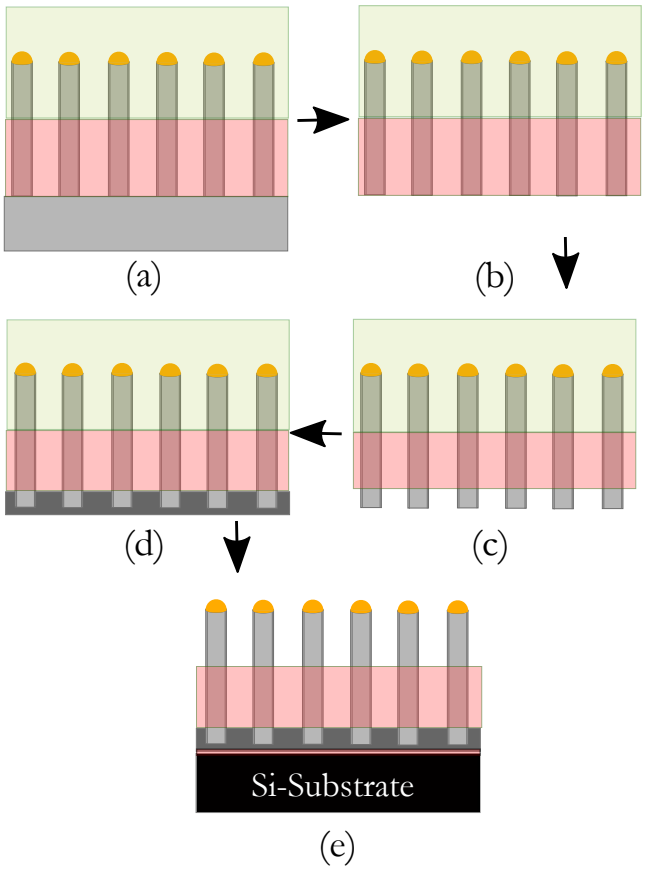

Figure 4.5: Initial process flow for 2 layer peel off. (a) A thin supportive layer is deposited before FC is applied on top. (b) The entire structure is peeled off. (c) The supportive film is etched back approximately 300 nm. (d) ITO is deposited as a back contact. (e) The sample is glued onto a Si-cell and FC is selectively wet etched, leaving a supportive polymer film around the nanowires.

4.2.1 Two Layer Peel-Off

Tu7 and S1813 were deposited onto nanowire samples with oxide films as described above. The supportive layers where etched down to reveal 700-800 nm of the nanowires on the S1813-sample and 500-600nm on the Tu7-sample after which FC was deposited as described in section 2.5 and left to dry for 48 hours before peel

off. The difference in revealed nanowire length was due to difficulties in controlling the etching process. The two layer peel-off was done with a FC film that did not contain any supportive mesh.

Peeling with a supportive layer proved to be more difficult than with only a FC layer. The adhesion between the supportive polymers and the substrate seemed to be higher than between the FC-film and the middle layer. When peeling the S1813-sample, only small patches containing nanowires followed. The sample with Tu7 gave better results, especially when utilizing the peel off with a small knife to lift the polymer film from the underlying substrate. Some areas on this sample were completely ripped off, while some areas still remained on the substrate. SEM images of the substrates after the two layer peel off can be seen in figure 4.6. Figure 4.6a shows how most of the nanowires remain on the substrate for the sample with the S1813 sample as supportive layer. Figure 4.6b illustrates both successful and unsuccessful peel off across the sample with Tu7. In the sample with S1813 the nanowires seem tilted inside the polymer as seen in figure 4.6a.

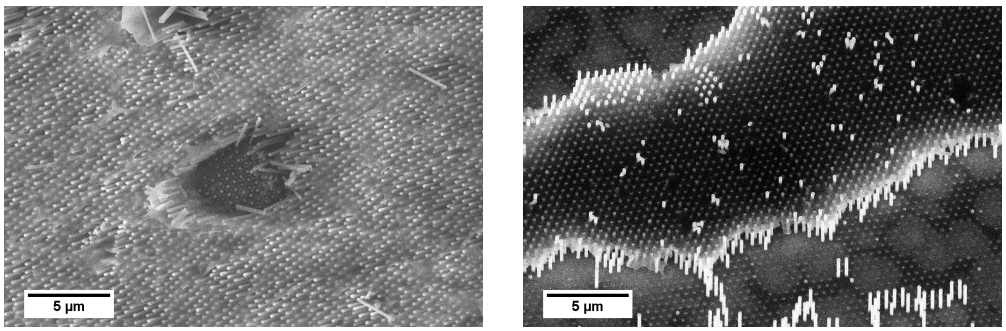

(a) S1813 supportive layer (b) Tu7 supportive layer

Figure 4.6: SEM images of the substrates after two layer peel off with a supportive layer spun on the nanowire samples. (a) Image at 0 ° tilt to the normal to the plane. (b) Image at 30 ° tilt to the normal to the plane.

A similar procedure was also carried out using UV-curable tape instead of the FC film. The UV curable tape, otherwise used for dizing wafers, has very high adhesive strength and releases when treated with UV-light. In this design the supportive layer was not etched and covered the nanowires completely. The tape was then put on the sample and rubbed so that it would adhere well to the underlying polymer and make the nanowires break at their base. However, this method was unsuccessful since the tape did not adhere well enough to the underlying polymer for the sample to follow during peel-off.

4.3 Three Layer Design

The results from the two layer peel off motivated a change in design since the wires and the supportive layer did not follow in the peeling. A three layer structure

was suggested, comprising a 200-300 nm polymer sacrificial layer at the base of the nanowires, a supportive middle layer of approximately 700 nm and finally a thick layer of FC for peel off purpose. The aim with this design was to make the etching of the backside of the sample unnecessary and the peel off easier. The bottom layer needed to be easily removed and did not need good adhesion to the nanowires or the middle layer. It was crucial that both bottom layers could be deposited with a well-defined thickness.

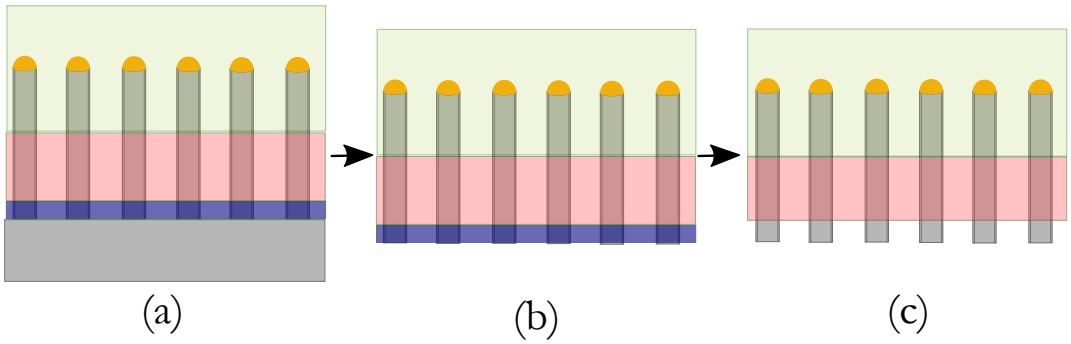

Figure 4.7: Illustration of the three layer design. a) Design before peeloff: a bottom sacrificial layer, a middle supportive layer and a top layer of FC for peel off. b) All layers follow in peel off. c) The sacrifical layer is easily removed to reveal the nanowire bottoms for metal deposition.

4.3.1 Chemical Resistance of Polymers

In the three layer design, the sacrificial layer needed to be removed without affecting the middle layer. It was also important that the sacrificial layer would be dissolved much faster than FC in the case that FC was dissolved by the same developer. Therefore the chemical resistance of the various polymers to some relevant solvents were tested. Samples with cured polymer films were put in the solvents for 5 minutes and they were inspected with SEM, if needed, to see the results. The results can be seen in table 3. Except the polymers that had been used earlier Poly(methyl methacrylate) (PMMA) was tested as a possible polymer to use as one of the films in the design presented in figure 4.7.

Table 3: Etch rates of polymer films.

	Solvent		
Polymer	FC Thinner	Acetone	MF-319
Tu7 (UV-Cured)	Withstands	Withstands	Withstands
S1813 (UV-Cured)	Dissolves	Dissolves	Dissolves
FC Film	Dissolves	Dissolves	Withstands
PMMA	Dissolves	Dissolves	Withstands *

*The results showed no significant removal of PMMA in MF319 even though MF319 should be able to dissolve PMMA according to literature and previous research [42, 43].

From the data in table 3 it was concluded that S1813 might be used as a sacrificial layer in combination with Tu7 as the middle layer. S1813 could be removed using MF319 without removing neither Tu7 nor FC. FC is dissolved in acetone, but a couple of minutes is not enough to dissolve the entire film. However a 2 μm thick PMMA-film disappeared quickly. Thus, dissolving a sacrificial layer of PMMA with acetone was seen as a possibility and therefore combining PMMA as a sacrificial layer and Tu7 as a supportive layer was a possible alternative to combining S1813 and Tu7.

4.3.2 PMMA as a Sacrificial Layer

PMMA was investigated as a sacrificial layer since PMMA is easily removed using acetone or another positive resist remover. It is also extensively used in the clean room and can be spun to a variety of thicknesses. Since PMMA is brittle the possibility of it cracking during peal off made it suitable as a sacrificial layer but not for support.

A range of different PMMA solutions were tested. There is a large selection of molecular weights and the percentage of solids in different PMMA solvents. For example, "950 PMMA A2" has 2% of solids dissolved in anisole (A) and a molecular weight of 950,000. To find a suitable polymer solutions to be used as a sacrificial layer several solutions were tested at different spin speeds as seen in table 4.

There were three clear results from spinning PMMA onto samples with vertical nanowires. The nanowires could be completely covered, as was seen with the polymers described in section 4.2. In other cases, the PMMA sometimes partially covered the nanowires and climbed on the walls of the nanowires as illustrated in figure 4.1. The third result was that the nanowires bent and clumped together in bunches of around 10-30 nanowires as PMMA with medium high viscosity sunk down between the nanowires. The investigated settings are given in table 4. Spinning 950 PMMA A6 gave a 3 μm thick film of PMMA while spinning 950 PMMA A2 and 200 PMMA A5.5 at 3000 rpm gave approximately 200 nm thick coatings that climbed on the nanowire walls. The remaining settings resulted in bunched and broken off nanowires and were therefore not suitable. Etching PMMA in RIE is very slow. The etching rate is approximately 2 nm/s and to etch down a 3 μm thick film to 300 nm took around 20 minutes. Moreover, the measured etching rate as seen in table 2 varies significantly and have a standard deviation in the same order as the rate itself. Thus, the obtained thickness after 20 minutes of etching would be very hard to predict and might result in the complete removal of the film. It was therefore preferable to etch a PMMA film that had a thickness close to 300 nm. Spinning 200 PMMA A5.5 at 3000 rpm gave the most consistent results and from this point on this solution was used.

Table 4: The PMMA solutions tested at different spin speeds and the resulting film: ○: 200-300 nm thick coating with climb. ●: 3μm thick film, X: Bunched and tilting wires.

	Spin Speeds				
PMMA solution	2000	2500	3000	3500	5000
950 PMMA A2	X		○	X	
950 PMMA A4		X	X	X	X
950 PMMA A6		●	●		
950 PMMA A8	X		X	X	X
200 PMMA A5.5			○		

To obtain a 300 nm thick PMMA film, 200 PMMA A5.5 was spun on to the sample 3 successive times at 3000 rpm during 60s. Each additional deposition of PMMA added approximately 100 nm of PMMA-film. The sample was baked for 5 minutes at 160 °C after the final deposition. After this, the sample was etched in the RIE at 150 mTorr and 40 W with an O_2 flow of 40 sccm during 30 s to investigate if it was possible to remove the polymer solution that had climbed up the walls of the nanowires. SEM observations showed that this gave a final thickness of PMMA of 200-300 nm and very little climbing of PMMA was seen.

4.3.3 Three Layer Peel-Off

Two samples with three layers were prepared for peel off. Both samples where 11x9 mm, had approximately 2μ m long nanowires grown without any SiN_x mask and had an oxide cover. Sample 1 had a sacrificial layer of S1813. S1813 was deposited in the same way as in the two layer design, namely by spinning at 3000 rpm for 60s, followed by baking at 90 °C for 60s and then 200 °C for 20 minutes. This film was etched down during a total of 1200s to cover around 300 nm of the nanowires. Sample 2 had a sacrificial layer of PMMA. 200 PMMA A5.5 was deposited and baked as described in section 4.3.2 to obtain a film of an approximate thickness of 400 nm and was etched for 30s to reduce the PMMA that climbed up on the walls of the nanowires. The final thickness was 200-300 nm. Both of these samples where covered with Tu7 using the same method as when deposited in the two layer design. After baking, the Tu7 was UV-cured for 25s and etched down using RIE to reveal approximately 900-1000 nm. The final thickness after every etching step was determined by imaging the sample in the SEM at 30 ° towards the normal of the plane. More edge effects from the spinning were seen in Sample 2, resulting in a larger relative area of the sample with ticker Tu7-film and nanowires that were not revealed after etching. Finally a FC film was applied and after 48 hours of drying peel off was performed.

After peel off, the next step was to remove both sacrificial layers. Sample 1 was UV-treated for 15s in soft UV from the backside of the sample now consisting of nanowires embedded in polymer films. This weakened the S1813 and the sample was put in MF319 for 3 minutes for removal of the sacrificial layer. Sample 2 was put in Acetone for 2 minutes to remove the PMMA. In sample 2 the FC film clearly started to dissolve. The time in which it was exposed to acetone was, however, not enough to cause any significant reduction in FC film thickness, although the

film became very uneven. After letting the FC film dry out in an oven and a low pressure chamber, the films of both samples lay flat. The samples where inspected in the SEM before and after the removal of the sacrificial layer was performed and showed that no significant length of the nanowire bases were exposed. Sample 1 was once again treated in UV- light and MF319 and Sample 2 was re-treated in both acetone and later in MF319 to remove PMMA. However, the bases of the nanowires were still not exposed. Hence, the samples were instead etched from the back side in RIE, with the settings used for Tu7 etching as mentioned in section 4.3.1 for a total of 600 s. This exposed between 300-500 nm of the backside of both samples. This was followed by the sputtering of 25/600/25 nm of Ti/Au/Ti after which the samples were put in FC thinner for 48 hours.

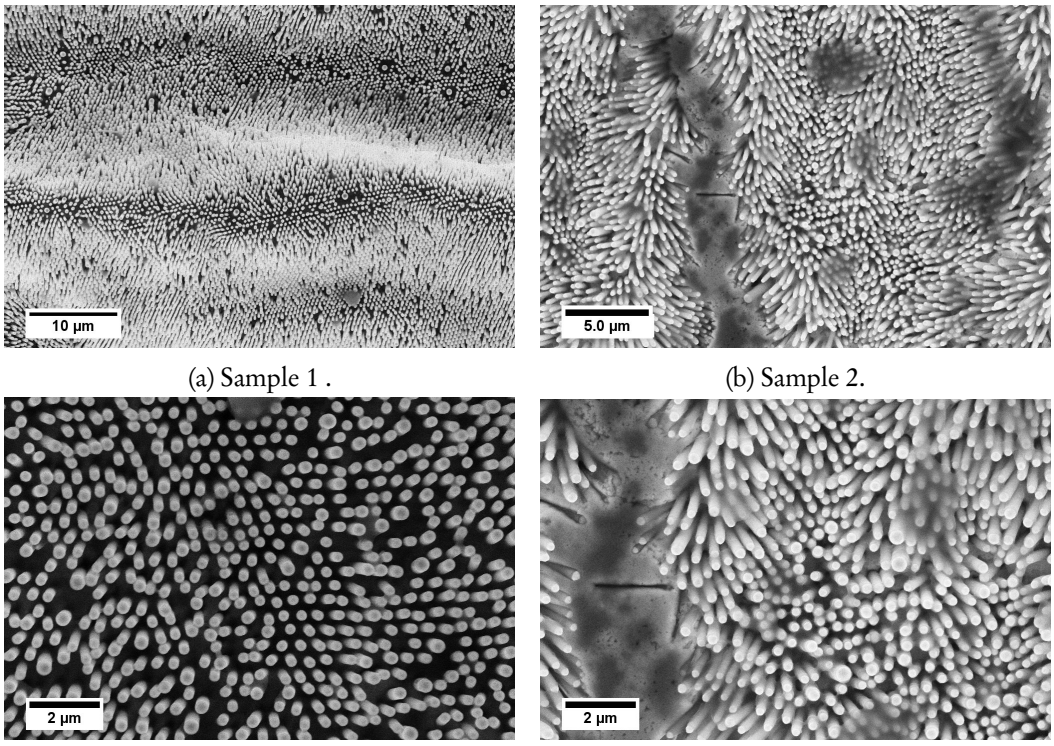

(a) Sample 1 .

(b) Sample 2.

(c) Sample 1.

(d) Sample 2.

Figure 4.8: SEM images of the samples with a three layer design after peel-off. Sample 1 with a S1813 sacrificial layer and Sample 2 with a PMMA sacrificial layer. All images are after deposition of a metal backing and dissolving of FC for 48 hours.

Images of Sample 1 and 2 after peel off, RIE and after FC has been dissolved can be seen in figure 4.8. Inspecting the substrates after peel off showed that only very short stubs of a few nanometers was left from the peeled off nanowires on the substrate.

The peel off of Sample 1 required a relatively high amount of force and as a result the FC film stretched out significantly during the process and became uneven. However, during the drying out of FC, this sample seemed to shrink and

flatten. As seen in figure 4.8c which was taken at 0 ° there are nanowires standing vertical on the sample. However, there are also large areas in which the nanowires are tilted. Figure 4.8a shows how the film has formed a wave-like structure while contracting during the dry-out.

Sample 2 was easier to peel off but a smaller number of nanowires followed the film than for Sample 1. This was probably due to the Tu7-film being thicker along the edges of this sample. The polymer film obtained a lot of cracks during peel off and more nanowires where left on the substrate compared with sample 1. After the samples were taken out of the thinner to dry, it was seen that Sample 2 still had a lot of FC residues. Moreover, the nanowires tilted significantly more and the sample was falling into little pieces. Due to its fragility it could not be put back into the FC thinner in order to remove the residual FC film. Figure 4.8d shows how one of the cracks exposes the metal backing. It was not possible to apply a top contact because of electrical short circuiting.

From the results after peel off of Sample 1 and 2 the conclusion was drawn that S1813 was more suitable as a sacrificial layer for the following reasons. First, since the film is around 2 μm after deposition, the uniformity of the S1813 film can be examined before etching down the film to its desired thickness. Moreover, the etching rate of S1813 is more consistent and predictable compared to PMMA. The removal of PMMA with acetone is problematic, since the first contact film quality is affected and MF319 did not seem to remove PMMA, just as was mentioned in section 4.3.1. Finally, the peel off with a bottom coating of S1813 required less force than when using PMMA.

Since there were very few missing or fallen nanowires, it was concluded that the nanowires seem to have obtained some support from the middle layer even though the polymers were significantly stretched out during peel off and the nanowires were not standing vertical. The tilting of the nanowires was mainly attributed to the fact that the polymer film was far from flat after peel off. Due to lack of suitable samples, this peel off was done with samples without a SiN_x mask on the substrate which had previously been shown to be crucial for successful peel off [27].

The main problem in the three layer peel off was that the bottoms of the nanowires were not exposed after the attempted dissolving of the sacrificial layer. When developing the method of coating the sample with a 300 nm thick layer of S1813 and PMMA, cross sectional images of the samples were taken to investigate the final results. However, this required a small piece of the sample to be cut off with the risk of harming the samples. Furthermore, a smaller sample was harder to peel off compared to a normal sized sample of 11x9 mm. Therefore the thickness of the sacrificial film for Sample 1 and 2 was determined by imaging from above at 30 °. The polymers are insulating materials that are hard to image in an electron microscope, making the edge of the polymer very hard to see in the SEM. The top of the sacrificial layer was therefore estimated to be where the image of the nanowires becomes less sharp and the thickness therefore had a high degree of uncertainty. Moreover, Even if the PMMA was hard baked before Tu7 deposition it was possible that the Tu7 solution had slightly dissolved the PMMA and penetrated into the film. This is since Tu7 and PMMA both have the same solvent; phenyl methyl ether. If this was indeed the case, there was a mixture of PMMA and Tu7 in the

bottom sacrificial layer in Sample 2, which would explain why it did not dissolve as expected. Since PMMA also was subjected to UV light during the treatment of Tu7, any Tu7 incorporated in the PMMA film would also be treated and become resistant to most solvents. The S1813 was not UV-treated before Tu7-deposition to ensure that it was as chemically stable as possible. Still, some mixing may have happened at the surface and if the film was thinner than what was thought from the SEM-images, Tu7 may have reached through the entire film.

From these results it was decided that for further peel off, PMMA was not suitable as a sacrificial layer. Moreover, a thicker layer of S1813 was to be used to ensure no mixing of polymers. A sample with SiN_x mask was to be peeled off to make the peel off easier and the stretching of the film was to be minimized if possible.

4.3.4 Incorporation of a Mesh

As mentioned earlier, the nanowires were often tilted after peel off probably because of significant stretching of the polymer membrane during the process. By incorporating a mesh into the membrane the stretching was minimized. The mesh was supplied by Photonic Cleaning Industries as a supplement to FC and consisted of a rigid but thin fabric.

Two different designs for how the mesh could be incorporated in the peel off film were tested. In the first method a partial mesh was used in which a hole was cut in the mesh so that only the outer parts of the sample were covered by the mesh. Following this, two layers of first contact polymer was applied with a 15 minute pause between applications. In the second approach one layer of first contact polymer was applied after which the entire sample was covered in a complete mesh and a final layer of first contact polymer was deposited. The two different designs can be seen in figure 4.9.

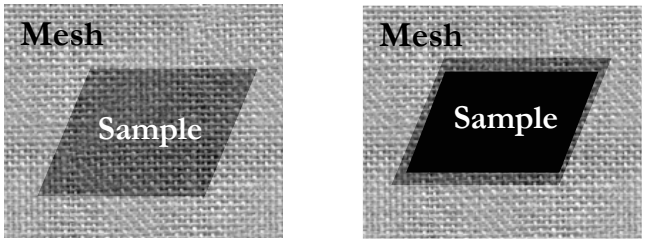

Figure 4.9: Illustration of incorporation of the mesh into the peel-off film. (a) Complete mesh covering the entire sample. (b) Partial mesh with a hole over the sample.

Peeling off with a partial mesh was complicated since the film had a tendency to break at the inner edges of the mesh. Moreover, the polymer film was still stretched in the center of the sample. These problems indicated that this design was not suitable for peeling off larger samples.

Peel off with a complete mesh and a single layer of FC was substantially easier than using a partial or no mesh. The film peeled off using less force and it showed

no significant stretch. Moreover, the film was flat after peel off, which was usually not the case otherwise. When peeling with a complete mesh the nanowires still broke at the desired location, at the bottom close to the substrate, leaving short stubs on the substrate. Only a few more nanowires where left on the substrate as compared to previous peelings without the mesh. However, after 600 s of RIE of the sample's backside to reveal the nanowires embedded in FC, it was observed that the nanowires were still tilted to a great extent, as seen in figure 4.10. The amount of tilting of the nanowires was unexpected considering that the film was from a macroscopic view not stretched out at all during the peel off. However, it is possible that on a microscopic scale the FC film stretched out during peeling due to adhesion to the substrate. This might cause permanent tilting of the nanowires in the film. Still, it is recommended that a complete mesh be incorporated into the standard design for any peel off using FC.

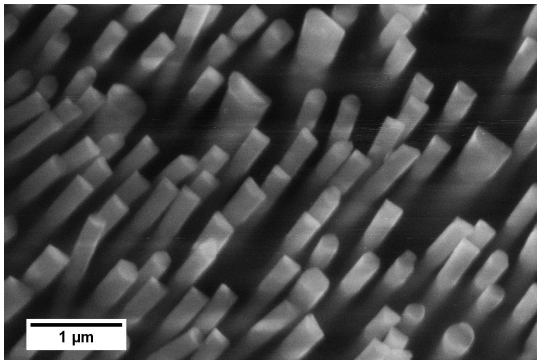

Figure 4.10: Top view of the backside of peeled off sample with complete mesh after 600 s of RIE to reveal the bottoms of the nanowires.

Next, a complete mesh was incorporated into the FC film in a three layer design. The sample had approximately 400-500 nm sacrificial layer of S1813 and a supportive layer of Tu7 which was etched down to reveal 900-1000 nm of the nanowires. Both the film of S1813 and Tu7 were deposited in the same way as described in section 4.3.3. The sample had oxide coated nanowires and were grown on a SiN_x-coated substrate.

The three layer peel off with a complete mesh was entirely unsuccessful. No nanowires followed in the peel off and only the FC film with its mesh was peeled off from the sample. The peel off of a sample with a SiN_x mask was expected to be easier than without the mask, based on previous work [27]. However, when peeling this three layer sample the FC-film loosened easily and no part of the underlying sample followed. In contrast to FC, S1813 might have lower adhesion to a substrate without the SiN_x mask than to a substrate with the mask. Since the peel off using a compete mesh was substantially easier than without it, the unsuccessful peel off with the three layer design in section 4.3.4 was first and foremost attributed to the interaction between the S1813 and the substrate.

4.4 Breaking nanowires by use of an Ultrasonic Bath

In the original method the nanowires were broken before peel off by swiping the sample with a tweezer from above by hand and it was not possible to perfectly reproduce this procedure (see section 2.5). Neither was it known if the swiping breaks off all the nanowires completely. Hence, it was investigated whether the nanowires could be broken off by ultrasonic treatment.

In an ultrasonic bath a specimen was placed in a liquid which was flooded with high frequency sound waves. This treatment was generally used for cleaning off adhesive contaminants. By applying moderate power, the nanowires were expected to break at the point with most strain; namely at the interface between the nanowires and their substrate.

Samples of as grown nanowires without any polymer film were put in beakers with either acetone or the remover MF319 which were placed in ultrasonic baths. Both samples were subjected to a power of 8 out of 10 during 3 minutes. The results showed that all nanowires were broken off at the base, leaving very short stubs.

Next, a sample of nanowires with $AlOx/SiO_2$ coating covered in FC with a complete mesh was put in in a ultrasonic bath before peel off in order to break the nanowires at their base. The sample was treated with an ultrasonic power of 8 out of the maximum setting of 10 for three minutes in MF319. However, the ultrasonic treatment did not result in an easier peel off. It was only successful in limited areas of the sample and many nanowires were left on the substrate as can be seen in figure 4.11.

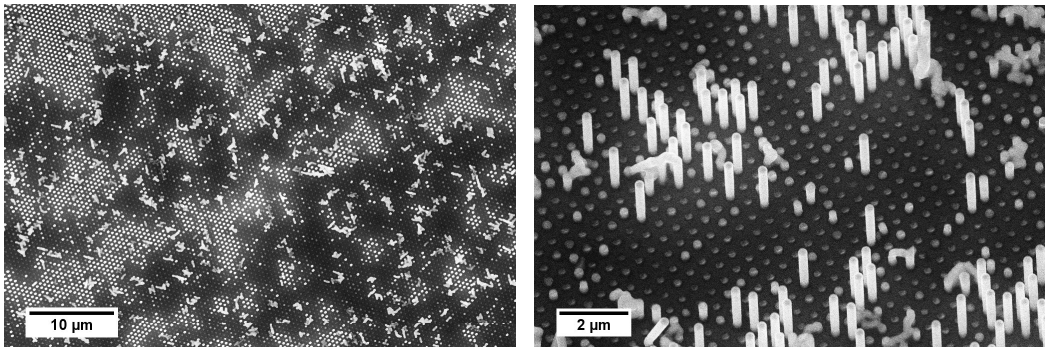

(a) (b)

Figure 4.11: Images of the substrate after peel off with a single layer of FC and a complete mesh and Ultrasonic treatment for 3 minutes.

The treatment in a ultrasonic bath may be a possible path forward, but more tests are needed. As seen in the SEM images, many nanowires have broken at the desired location. Possibly just an increase in power and/or the length of treatment would suffice to break all nanowires at their base. The testing of more settings could indicate whether ultrasonic treatment might be a suitable path forward. No more samples were available within the scope of this project.

A possible alternative method to the ultrasonic treatment would be to use a roller to roll across the sample. During nanoimprint a roller could be used to press the mold onto a sample. Such a roller could provide a well-controlled force [44]

and might therefore be suitable for the purpose of evenly breaking the nanowires.

4.5 FC Vacuum Compatibility

Partway through this project, at the start of the attempt to use the three layer design it was discovered that the FC film caused increased pressure in the main chamber in the SEM. The sample that was studied at the time had a FC film which had dried out during 48 hours but had not been baked at any elevated temperature. To enable further analysis of nanowires embedded in the FC, the outgassing of FC needed to be minimized. The working pressure in the sample chamber in the SEM needs to reach below 2×10^{-6} mBar within two minutes after introducing the sample to ensure that the SEM was not contaminated during imaging. However, FC was outgassing to such an extent that the pressure stabilized around 2×10^{-5} mBar. Such a high pressure in the main chamber eventually leads to contamination of the electron gun and the vacuum gauge which ultimately clogs up the SEM. By reducing the excess solvent in the FC film, the outgassing of FC was lowered.

By baking the sample at 80 °C over night (14 hours) the solvents from the sample were dried out so that the chamber pressure in the SEM reached 10×10^{-6} mBar in two minutes after introducing the samples. Next, the sample was put in another vacuum chamber to "pull out" any remaining solvents from the film. After keeping the sample in a chamber with a pressure of 0.08 mBar for 4 hours the pressure in the SEM reached 2×10^{-6} mBar with the sample in the chamber within 2:20 minutes which was thought as good enough to proceed imaging. From this point, any samples with FC were baked over night and dried out at low pressure prior to further treatment. This requirement substantially slowed down the device fabrication.

5 Electrical Characteristics

5.1 Contacting Solar Cells

In tandem solar cells the individual units can either be connected in series or in parallel. Generally, the series structure is more common since it is easier to build [45]. When connected in series through a two terminal design the cells are separated by a recombination layer and the currents through both cells need to be equal which sets constraints on the bandgaps of each cell but with the advantage of voltage addition. The four-terminal design (fig5.1 gives the freedom of connecting the cells in either series or parallel and the two cells are separated by a dielectric layer which lies between their separate transparent electrodes. If connected in parallel, the individual currents of each cell is summed and the need for current matching of each cell is eliminated. However, since the total voltage output in a serial connected structure is the sum of the separate cells this value is higher than for the parallel structure in which the output voltage is given by the individual cells.

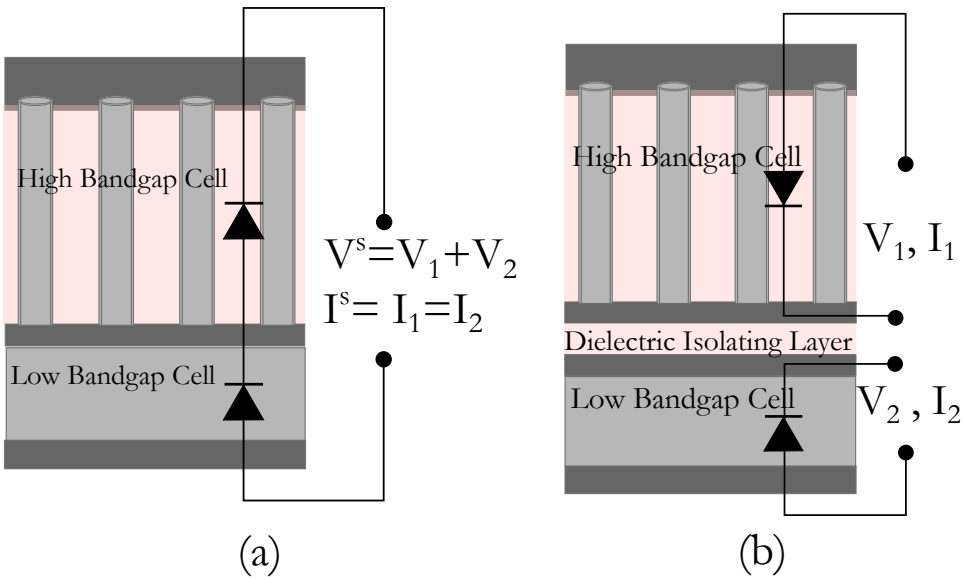

Figure 5.1: Schematic image of (a) A two-terminal series tandem structure (b) A four-terminal parallel structure

A clear advantage of using a two terminal structure is the problem of producing laterally conductive and transparent middle electrodes between each sub cell in the other design. However, as shown by Etxebarria et al.[46], serial connected cells gives a higher efficiency for a given material combination in which currents are matched but since the parallel contacting allows for a combination of materials with higher bandgap differences this design ultimately results in higher efficiency [45, 46, 47]. In the four-terminal design the operating points of both cells can be independently monitored to ensure maximum power output at any point of operation. Moreover, the dielectric insulating layer between the cells in the four terminal design can be deposited to a desired thickness that allows for light coupling

into the second cell [48]. Finally, the four terminal approach allows for mechanical stacking of cells when epitaxial growth of stacked cells is impossible or when a good electrical contact to both cells through a single contact cannot be achieved. Finally the four-terminal design allows for placing a peeled of nanowire solar cell onto planar cells already in use, making this more commercially applicable.

To determine the ultimate structure for our solar cell devices we needed to evaluate the electrical contact between the p-segment in the nanowires and the p- doped unit underneath. As an initial step the aim was to evaluate the contact between the peeled off nanowires and a sputtered back contact of metal or ITO. These measurements were done using a conductive Atomic Force Microscope. Even if the peel off process did not give perfect results the electrical measurements were done to give an indication as to what kind of tandem design was most interesting.

5.2 Ohmic Contacts

An ohmic contatc between a metal and a semicondutor is a contact with negligible resistance and such a contact is desirable between the nanowires and the back contact. To obtain a perfect ohmic contact, band continuity between the semiconductor and the metal is required, meaning that these have equal work functions. The work function of a material is the energy difference between the electron at the highest occupied energy level in the material (the fermi level) relative to vacuum [15]. In most cases, the difference in work function between two materials results in a potential barrier at the interface, i.e. a so called Schottky barrier in which current will only flow if the voltage reaches over a threshold value. The quality of the contact can be improved by increasing the doping concentration or by annealing which causes any surface oxide states to diffuse away from the surface and which removes any dangling bonds by inter diffusion of the metal and semiconductor [49] .

Close to the surface, on the semiconductor side there will be a region depleted of charge carriers due to a built in voltage [15]. By heavy doping of the semiconductor this depleted region becomes thinner and one achieves a tunneling junction in which the wave nature of electrons allow them to tunnel through the potential barrier. This contact is generally most easily obtained in junctions with a n-doped semiconductor. However, this is material dependent and GaAs, for example, is more easily contacted if it is p-doped [27].

Ohmic-like contacts to n-InP are rather easily obtained while contacts to p-InP are more complicated due to the much higher metal barrier height and the low mobility of holes in p-InP because of their high effective mass [50]. In general, p-InP form Schottky barrier contacts to most metals [51]. However ohmic-like contacts to p-InP are achievable with gold alloys and the contact resistance is lowered greatly by annealing above 300 $^{\circ}C$ [51, 52]. The current-voltage characteristics of an ITO/p-InP contact have showed to be improved by high doping concentrations and annealing at temperatures above 200 $^{\circ}C$ [53]. While research has shown that p-type Si films deposited on ITO forms a nearly ohmic contact [54], the contact between p-doped nanowires of InP and ITO is still not well defined. A Schottky contact to the InP nanowires needs to be avoided and if a good enough contact

between InP and ITO cannot be achieved, ZnO may also be considered as a transparent back contact to p-InP. However, ZnO forms a Schottky contact to silicon [55, 56] and a four terminal design would then be required, using ITO as the top contact on Si. If ITO forms an adequate contact to p-InP, there will still be the possibility of choosing between a two- or four-terminal design later on.

It is crucial that a high enough current can run through the contact between the nanowires and the back contact. To get an idea of the current that each nanowire might generate, some simple assumptions can be made. For a nanowire array of 200 nm diameter nanowires with a 500 nm pitch, the areal number density of nanowires is around 4.9×10^{13} m^{-2}. The sun delivers a constant average power of 1360 W m^{-2} on earth, which results in each wire receiving a power of 2.78×10^{-11} W. Previous research on solar cells using InP nanowires have shown a open circuit voltage of 0.779 V [5]. In an ideal cell, the open circuit voltage would also be the output voltage. Assuming a solar cell efficiency of 14%, the expected current through a nanowire is derived from the voltage of 0.779V and power input of 2.78×10^{-11} W to be $I = 5.0 \times 10^{-12}$ A. Thus, to work as an adequate solar cell, the contact to the bottom segment of p-InP nanowire needs to be able to deliver such a current.

5.3 Experimental

5.3.1 Sample for cAFM

2 μ m long p-i-n doped InP nanowires with the p-segment in the bottom part of the wires were studied. The inspected samples had unevenly sized nanowires because the gold particles seeding the nanowires were poorly defined. Electrical measurements were done on the normal-sized nanowires. Two samples were prepared, one with a titanium and gold back contact and one with a ITO back contact. As mentioned in section 5.2 the current through a p-InP/gold-contact was more easily predicted and was therefore chosen as a sample to image as a proof of concept for this imaging method.

The samples were prepared in the same way as in the initial process flow at the start of this project as shown in figure 2.8. As grown nanowires were covered in FC and were peeled off, 300 nm of FC was etched back using the RIE after which 25/600/25 of Ti/Au/Ti was deposited on one of the samples. The thin layer of titanium was used to avoid the diffusion of gold into the nanowires. 300 nm of ITO was sputtered onto another sample. No planarizing layer was applied but the sample was of free standing nanowires supported by a metal backing. To obtain a good electrical contact to the nanowires the gold tips were not removed and the sample was placed on a copper (Cu) coin.

To obtain a good electrical contact to the sample, it was crucial that there was a good contact between the metal back contact deposited on the wires and the copper coin which was used to mount the sample in the cAFM. The sample could not be glued down with PDMS which had previously been used as a bonding matrix [27] due to the risk of creating an insulating layer between the copper and the sample. To be useful as a means of bonding the sample to the Cu-coin, any bonding method needed to be chemically resistant to the FC thinner, since this was used to dissolve

FC to expose the gold tips of the wires. Several types of sticky tape as well as silver glue showed to loosen or dissolve from their surfaces when immersed in FC thinner and were therefore abandoned as a means of holding down the samples on the copper coin.The final solution was to physically hold down the samples on the coin using the peel off mesh with a hole in the middle to make sure not to touch the center nanowires on the sample. A metal ring was put on the remaining mesh as a weight to keep the sample down while immersed in thinner. After dissolving the FC the sample stayed put on the copper coin. It was flat and had good enough adhesion to the coin not to move and it was inspected in SEM to find an area with nanowires that were standing up vertically.

As seen in figure 5.2, showing the sample with metal backing, the nanowires were tilted after peel off. This is undesirable in any final structure but the sample was still considered good enough for doing electrical measurements.

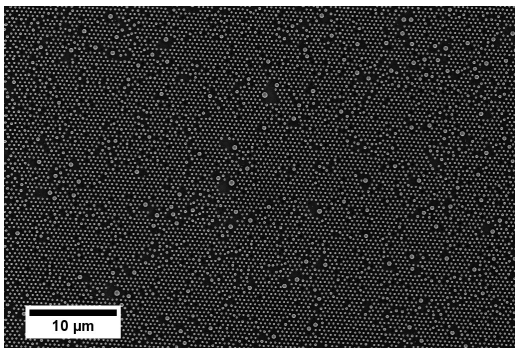

(a) Before peel off

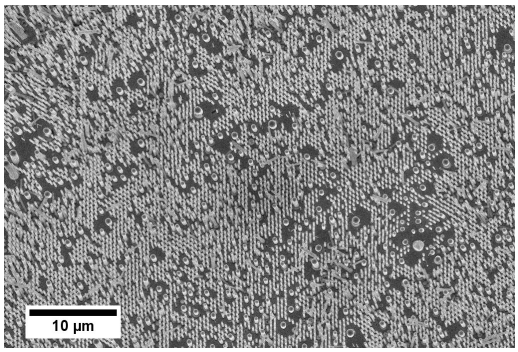

(b) After peel off

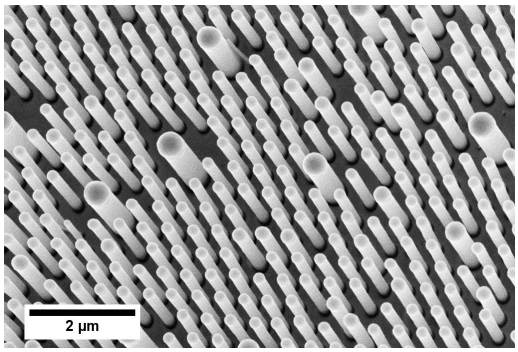

(c) After peel off

Figure 5.2: Top view SEM-images of the sample studied in the cAFM with metal backing before (a) and after (b and c) peel off.

5.3.2 cAFM Measurements

An AFM-probe of a platinum-iridium alloy was used to do a full scan in contact mode. The sample studied was the one imaged in figure 5.2. The sample had a large number of fallen nanowires and obtaining a topological image in which the gold particles could be distinguished was difficult. Thus, a constant voltage of 3 V was set across the sample. This enabled localization of the gold particles that were electrically connected with the underlying copper coin through the nanowire. After this, a voltage sweep could be done by placing the probe on one of these gold particles.

5.4 cAFM Results and Discussion

The images obtained from a contact mode scan in which a voltage bias of 3V was applied across the sample can be seen in figure 5.3. This was the only scan that could be made due to a breakdown of the module operating the conductivity measurements in the AFM. As seen in figure 5.3a the topographical image obtained in contact mode does not show evenly spaced nanowires in an array. Moreover, the limited vertical reach of the cantilever prevents any true value of the nanowire height being obtained. It is worth remembering that the nanowire diameters were approximately 200 nm. The big bright area in the center of figure 5.3a is bigger, suggesting that this nanowire is most likely one of the bigger nanowires as seen in figure 5.2 . If the nanowires had been standing perfectly vertical, only bright dots in a well defined pattern would have been seen. The AFM image indicates that the nanowires were tilted.

The current map in figure 5.3b gives complementary information to the height measurement. The bright spot close to the center of the image shows where a higher current of around 200 pA ran through the nanowire. This was a spot suitable for lowering the probe and ramp up the voltage to obtain a current-voltage curve. However, this could not be done due to the breakdown of the AFM. Still, the resulting image illustrates that a contact to p-type InP was achieved.

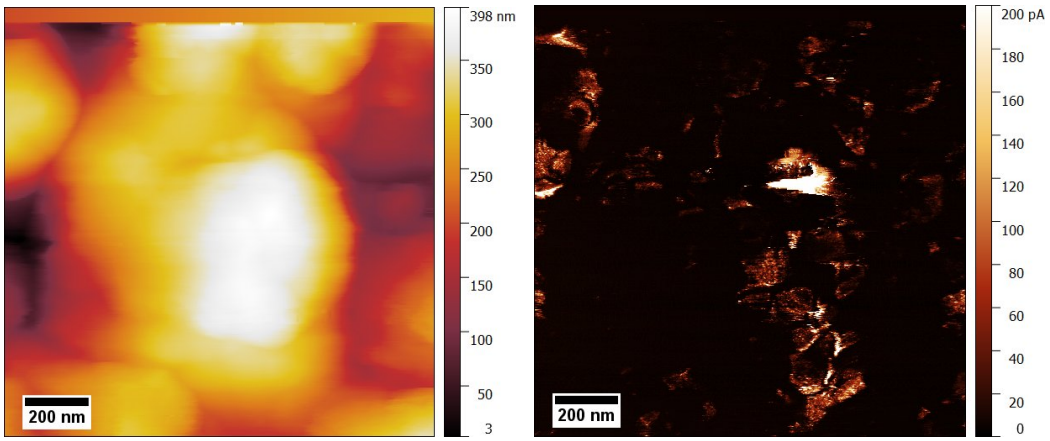

(a) Height Measurement (b) Current Measurement

Figure 5.3: Images obtained in the first full scan, operating in contact mode with a voltage bias of 3V between the tip and the sample.

The results presented in this section indicate that performing probe measurements to obtain the IV-characteristics in vertical nanowires is feasible using a cAFM. It was possible to localize a gold particle and make a conductivity map of the sample. Moreover a contact to p-type InP has been achieved via a sputtered metal contact without any post processing. The current observed reached well above the expected current per nanowire in a solar cell. Thus, these measurements show promise for future investigations on ITO-contacting to such nanowires and for the characterization of the diode characteristics of the nanowires. However, it should be noted that the voltage set across the wire is several times higher than the open circuit voltage expected in the nanowires under illumination. In any future measurements, the current at around 0.7 V is of interest and measurements may also be done under illumination.

It should be noted that these nanowires did not have an insulating oxide layer. Hence, it is not known if the current is running solely through one single wire or if fallen wires that touched other wires on the sample contributed as an extra path for the current. This would mean that the metal/wire- contact cannot be known to correspond to one single nanowire. An oxide layer is crucial for any further voltage-current measurements. This sample did not have isolated nanowires due to time restrictions during preparations of the first sample. Other samples with an oxide layer were prepared but were never imaged due to the breakdown of the cAFM.

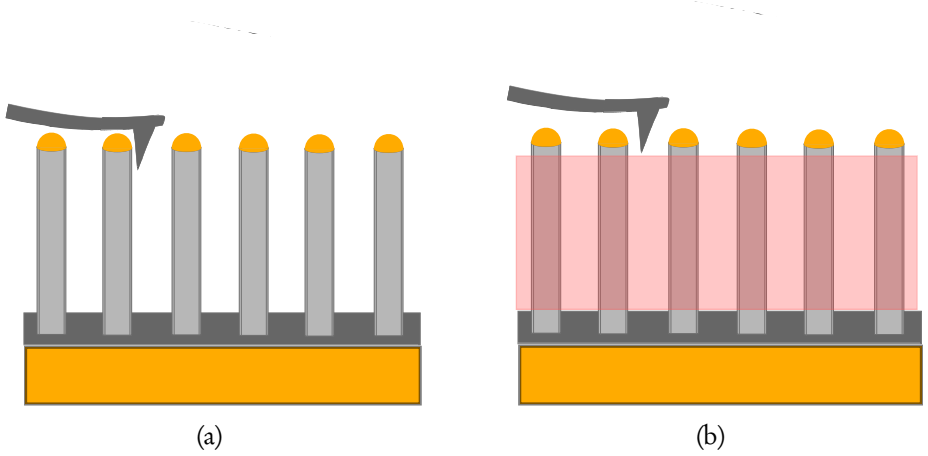

Figure 5.4: Improved sample design for contact mode AFM measurements. a) Illustrating the sample imaged in this project. b) Illustrating a sample with an etched down polymer layer to minimize the aspect ratio of the sample.

The image obtained above gives a poor view of the sample itself. To obtain a good image of nanowires with an aspect ratio as high as these nanowires had, non-contact mode with another cantilever should be used. However, the microscope cannot store the location on a sample if opening the AFM to change the probe to one designed for contact mode measurements. Therefore a non contact mode was never attempted. To obtain a better image using contact mode, a planar layer similar to the supportive layer of polymers seen in section 4 could be applied. This

would minimize the aspect ratio of the sample. Preferably, this layer layer would be thick enough to only expose the topmost part of the nanowires, as illustrated in figure 5.4. This would also protect the probe itself from crashing into nanowires during contact mode scans. Due to the limited feedback control of the AFM and the reach of the probe it is impossible to obtain true values for the topography of the sample. If the microscope had become functional again, such a polymer layer would have been applied before further imaging.

6 Summary and Outlook

This project aimed at developing a method in which arrays of nanowires with lengths around 2 μ m could be peeled off from their native substrate while keeping their array structure and their vertical orientation. The incorporation of a chemically resistant and supportive polymer film into the peel off film used to peel off the nanowires was attempted with some success. By combining three films to obtain a sacrificial bottom layer of S1813, a middle supportive layer of Tu7 and a FC ™ polymer peeling layer, a sample with nanowires supported by a polymer film was created. Moreover, attempts were made to minimize the stretching of the first contact film during peel off and to break the nanowires at their base in a consistent way.

Nanowire gold tips were successfully localized by the use of a conductive AFM. Furthermore, an cAFM image of a p-i-n doped InP-nanowire was achieved. This confirmed that the p-doped InP was successfully contacted to the back contact and that the wire could carry a significant current. Since no measurement with an ITO back contact was done, no conclusions about the choice of a two- or four-terminal design could be made.

For future development it is of interest to replicate the three layer peel off with a sacrificial layer of S1813 on a sample grown without a SiN_x mask but with a complete mesh to see if the adhesion of S1813 to SiN_x is low enough for peel off. Moreover stronger and longer ultrasonic treatment of polymer embedded wires might be investigated as an alternative method to breaking the nanowires by pressing from above with a tweezer. Possibly, the use of a roller, as mentioned in section 4.4 could be suitable for this purpose. Moreover it is of interest to cut through a three layer sample to obtain a cross sectional image to see if the separate polymer layers can be distinguished and if they are indeed of the thickness expected after spinning.

If the tilting of the nanowires after peel off cannot be minimized by the use of a mesh, a supportive layer or a standardizing of the breaking of nanowires, a new peel off polymer might have to be considered. It seems as if FC is stretching out at the interface between the polymer film and the substrate and it also needs to be extensively post baked before analysis. An alternative polymer which is flexible, adhesive and has low enough viscosity to penetrate between the nanowires is desirable. A polymer which might serve as a replacement for FC is polyimide which gives flexible and durable films of more than 90% optical transmission and shows good promise for flexible microelectronics [57]. Moreover, polyimide structures are usually formed through solvent casting and have been used for a similar purpose in peeling off graphene from it's growth surface [58].

Finally, more electrical measurements have to be done. A voltage sweep to obtain a IV-curve is required to characterize the electrical contact between the nanowire and the metal back contact. Since the final design is to have a transparent contact, focus should perhaps be put into investigating the contact between the nanowires and ITO or possibly ZnO.

References

[1] N. Anttu, A. Abrand, D. Asoli, M. Heurlin, I. Aberg, L. Samuelson, and M. Borgstrom, "Absorption of light in InP nanowire arrays," *Nano Research*, vol. 7, no. 6, pp. 816–823, 2014.

[2] I. Åberg, G. Vescovi, D. Asoli, U. Naseem, J. P. Gilboy, C. Sundvall, A. Dahlgren, K. E. Svensson, N. Anttu, M. T. Bjork, and L. Samuelson, "Gaas nanowire array solar cell with 15.3 % efficiency at 1 sun," *Journal of Photovoltaics*, vol. 6, no. 1, pp. 185–190, 2016.

[3] J. H. Davies, *The Physics of Low-dimensional Semiconductors*. Cambridge Books Online, 2012.

[4] N. Anttu, *Nanophotonics in absorbing III-V nanowire arrays*. PhD thesis, Lund University, 2013.

[5] J. Wallentin, N. Anttu, D. Asoli, M. Huffman, I. Aberg, M. H. Magnusson, G. Siefer, P. Fuss-Kailuweit, F. Dimroth, B. Witzigmann, H. Q. Xu, L. Samuelson, K. Deppert, and M. T. Borgstrom, "InP nanowire array solar cells achieving 13.8 % efficiency by exceeding the ray optics limit," *Science*, vol. 339, no. 6123, pp. 1057–60, 2013.

[6] "Nanowire-Based Tandem Solar Cells." [Online]Availible: `https://nano-tandem.ftf.lth.se/index.php`, Date accessed 2016-04-01, January 2015.

[7] Global Footprint Network, "World Footprint." [Online] Available: `http://www.footprintnetwork.org/en/index.php/GFN/page/world_footprint/`, Date acessed: 2016-02-24, 2015.

[8] D. Peterson, "Future world energy demand driven by trends in developing countries." [Online] Available: `http://www.eia.gov/todayinenergy/detail.cfm?id=14011`, Date Acessed: 2016-02-26, 2013.

[9] S. Xiao and S. Xu, *Status and Progress of High-efficiency Silicon Solar Cells*, book section 1. Springer Series in Materials Science, Switzerland: Springer, 2014.

[10] E. Martinot, "Renewables 2014 global status report," report, Renewable Energy Policy Network for the 21st Century, 2014.

[11] Energy Post, "Solar power passes 1 global threshold." [Online] Available: `http://www.energypost.eu/solar-power-passes-1-global-threshold/`, Date accessed: 2016-04-10, 2015.

[12] Center for Climate and Energy Solutions, "Outcomes if the U.N. climate change conference in Paris," in *COP 21*.

[13] E. Holthaus, "Our planet's temperature just reached a terrifying milestone." Feburary 2016, [Online] Available: http://www.slate.com/blogs/future_tense/2016/03/01/february_2016_s_shocking_global_warming_temperature_record.html, Date accessed: 2016-05-127, 2015.

[14] J. Trancik, "Technology improvement and emission reductions as mutually reinforcing efforts," report, Massachusetts Institute of Technology, 2015.

[15] M. Sze, S.; Lee, *Semiconductor Devices*. Whiley, third ed., 2013.

[16] M. A. Green, "Third generation photovoltaics: Ultra-high conversion efficiency at low cost," *Progress in Photovoltaics: Research and Applications*, vol. 9, no. 2, pp. 123–135, 2001.

[17] C. Honsberg and S. Bowden, "Silicon Solar Cell Parameters." [Online] Availible: http://www.pveducation.org/pvcdrom/design/solar-cell-parameters, Date accessed: 2016-02-20.

[18] A. Polman and H. A. Atwater, "Photonic design principles for ultrahigh-efficiency photovoltaics," *Nature Materials*, vol. 11, no. 3, pp. 174–177, 2012.

[19] W. Shockley and H. J. Queisser, "Detailed balance limit of efficiency of p-n junction solar cells," *Journal of Applied Physics*, vol. 32, no. 3, p. 510, 1961.

[20] Y. Xu, T. Gong, and J. N. Munday, "The generalized shockley-queisser limit for nanostructured solar cells," *Sci Rep*, vol. 5, p. 13536, 2015.

[21] H.-J. Choi, "Vapor-liquid-solid growth of semiconductor nanowires," in *Semiconductor Nanostructures for Optoelectronic Devices*, Nanoscience and Technology, Heidelberg: Springer-Verlag, 2012.

[22] K. A. Dick, "A review of nanowire growth promoted by alloys and non-alloying elements with emphasis on Au-assisted III–V nanowires," *Progress in Crystal Growth and Characterization of Materials*, vol. 54, no. 3-4, pp. 138–173, 2008.

[23] A. I. Hochbaum and P. Yang, "Semiconductor nanowires for energy conversion," *Chemical reviews*, vol. 110, no. 1, pp. 527–546, 2009.

[24] Lund University, "Nanowires with promise for photovoltaics - Magnus Borgstrom." 2014, Youtube, [Online], Available: https://www.youtube.com/watch?v=3LhsPtK60D0, Access date: 2016-05-05.

[25] E. L. Wolf, *Quantum Nanoelectronics: An Introduction to Electronic Nanotechnology and Quantum Computing*. Wiley, 2015.

[26] X. Dai, A. Messanvi, H. Z. Zhang, C. Durand, J. Eymery, C. Bougerol, F. H. Julien, and M. Tchernycheva, "Flexible light-emitting diodes based on vertical nitride nanowires," *Nano Letters*, vol. 15, no. 10, pp. 6958–6964, 2015.

[27] S. A. A. Abadizadeh, "Rip off and characterization of nanowire ensembles for photovoltaic applications," master of science thesis, Lund Univesity, 2013.

[28] V. Miikkulainen, M. Leskela, M. Ritala, and R. L. Puurunen, "Crystallinity of inorganic films grown by atomic layer deposition: Overview and general trends," *Journal of Applied Physics*, vol. 113, no. 2, pp. 02130101–021301101, 2013.

[29] G. S. May and S. M. Sze, *Fundamentals of semiconductor fabrication*. New York Chichester: Wiley, wiley international ed., 2004.

[30] H. H. Gatzen, *Micro and Nano Fabrication Tools and Processes*. Heidelberg: Springer Berlin Heidelberg, 2015.

[31] R. F. Egerton, *Physical Principles of Electron Microscopy*. Springer Science, 2005.

[32] J. Goldstein, *Scanning electron microscopy and X-ray microanalysis*. New York: Kluwer Academic/Plenum Publishers, 3rd ed., 2003.

[33] P. Eaton and P. West, *Atomic Force Microscopy*. Oxford University Press Inc., New York, 2010.

[34] T. Yang, S. Hertenberger, S. Morkotter, G. Abstreiter, and G. K., "Size, composition, and doping effects on In(Ga)As nanowire/Si tunnel diodes probed by conductive atomic force microscopy," *Applied Physics Letters*, vol. 101, no. 23, p. 233102, 2012.

[35] P. Deb, H. Kim, Y. Qin, R. Lahiji, M. Oliver, R. Reifenberger, and T. Sands, "GaN nanorod Schottky and p-n junction diodes," *Nano Lett*, vol. 6, no. 12, pp. 2893–8, 2006.

[36] Shipley, "Microposit s1813 series photo resists." [Online] Available: `http://engineering.dartmouth.edu/microeng/processing/lithography/S1800.pdf`, Date accessed: 2016-03-15.

[37] K. H.-S. a. B. K. Wehrspohn, R. B., *Nanophotonic Materials: Photonic Crystals, Plasmonics, and Metamaterials*. John Wiley and Sons, 2008.

[38] G. Mariani, A. C. Scofield, C. H. Hung, and D. L. Huffaker, "GaAs nanopillar-array solar cells employing in situ surface passivation," *Nat Commun*, vol. 4, pp. 1–7, 2013.

[39] A. Goodyear, V. Taylor, and M. Cooke, "Edge effects in plasma etching," report, Oxford Instruments.

[40] Y. Aberi, "Development of all dry nanoimprint lift-off process for growth of nanowires," masters thesis, 2013.

[41] E. Nakai, M. Y. Chen, M. Yoshimura, K. Tomioka, and T. Fukui, "Ingaas axial-junction nanowire-array solar cells," *Japanese Journal of Applied Physics*, vol. 54, no. 1, 2015.

[42] Micro Chem, "NANO^{TM} PMMA and Copolymer ." [Online], Availible: `http://www.microchem.com/pmma_faq.htm`, Date accessed: 2016-05-13, 2016.

[43] D. S. Bodas and S. A. Gangal, "Poly(methyl methacrylate) as for microelectromechanical masking material system (mems) fabrication," *Journal of Applied Polymer Science*, vol. 102, no. 3, pp. 2094–2098, 2006.

[44] H. Tan, A. Gilbertson, and S. Y. Chou, "Roller nanoimprint lithography," *Journal of Vacuum Science and Technology B*, vol. 16, no. 6, pp. 3926–3928, 1998.

[45] Z. H. Kafafi, R. Gehlhaar, D. Cheyns, L. Van Willigenburg, A. Hadipour, J. Gilot, R. Radbeh, T. Aernouts, and P. A. Lane, "Four-terminal organic solar cell modules with increased annual energy yield," vol. 8830, p. 88300I, 2013.

[46] I. Etxebarria, A. Furlan, J. Ajuria, F. W. Fecher, M. Voigt, C. J. Brabec, M. M. Wienk, L. Slooff, S. Veenstra, J. Gilot, and R. Pacios, "Series vs parallel connected organic tandem solar cells: Cell performance and impact on the design and operation of functional modules," *Solar Energy Materials and Solar Cells*, vol. 130, pp. 495–504, 2014.

[47] S. Reynolds and V. Smirnov, "Modelling of two-and four-terminal thin-film silicon tandem solar cells," *Journal of Physics: Conference Series*, vol. 398, p. 012006, 2012.

[48] S. Essig, S. Ward, M. A. Steiner, D. J. Friedman, J. F. Geisz, P. Stradins, and D. L. Young, "Progress Towards a 30% Efficient GaInP/Si Tandem Solar Cell," *Energy Procedia*, vol. 77, pp. 464–469, 2015.

[49] B. Sharma, "Fabrication and characterization of metal-semicondcutor schottky barrier junctions.," in *Metal-Semiconductor Schottky Barrier Junctions and Their Applications* (B. Sharma, ed.), Dehli, India: Springer, 2013.

[50] A. Baca, F. Ren, J. Zolper, B. R. D., and P. S. J., "A survey of ohmic contacts to III-V compound semiconductors," *Thin Solid Films*, pp. 599–606, 1997.

[51] T. A. Gessert, M. W. Wanlass, T. J. Coutts, X. Li, and G. S. Horner, "Aspects of processing InP-related solar cells," *Solar Cells*, vol. 27, no. 1-4, pp. 307–320, 1989.

[52] L. P. Erickson, A. Waseem, and G. Y. Robinson, "Characterization Of Ohmic Contacts To InP," *Thin Solid Films*, vol. 64, pp. 421–426, 1979.

[53] H. Thomas and J. K. Luo, "Electrical characterization of ITO/p-InP heterostructures," *Journal of Applied Physics*, vol. 73, no. 6, p. 3055, 1993.

[54] G. G. Pethuraja, R. E. Welser, A. K. Sood, C. Lee, N. J. Alexander, H. Efstathiadis, P. Haldar, and J. L. Harvey, "Current-Voltage Characteristics of ITO/p-Si and ITO/n-Si Contact Interfaces," *Advances in Materials Physics and Chemistry*, vol. 02, no. 02, pp. 59–62, 2012.

[55] M. Asghar, K. Mahmood, M. Faisal, and M. A. Hasan, "Electrical characterization of Au/ZnO/Si Schottky contact," *Journal of Physics: Conference Series*, vol. 439, p. 012030, 2013.

[56] L. S. Chuah, Z. Hassan, S. S. Tneh, and S. G. Teo, "Study of electrical characteristics of zno schottky photodiode on si substrate," *Microelectronics International*, vol. 28, no. 1, pp. 8–11, 2011.

[57] H. Ni, J. Liu, Z. Wang, and S. Yang, "A review on colorless and optically transparent polyimide films: Chemistry, process and engineering applications," *Journal of Industrial and Engineering Chemistry*, vol. 28, pp. 16–27, 2015.

[58] T. L. Chen, D. S. Ghosh, M. Marchena, J. Osmond, and V. Pruneri, "Nanopatterned graphene on a polymer substrate by a direct peel-off technique," *ACS Appl Mater Interfaces*, vol. 7, no. 10, pp. 5938–43, 2015.